

Recent results from Bonn-Gatchina partial wave analysis



Petersburg
Nuclear
Physics
Institute

A. Sarantsev

HISKP (Bonn), PNPI (Russia)

MENU 2010

May 31-June 4 2010; Williamsburg

Bonn-Gatchina partial wave analysis group:

A. Anisovich, E. Klempt, V. Nikonov, A. Srantsev, U. Thoma

<http://pwa.hiskp.uni-bonn.de/>



Bonn-Gatchina Partial Wave Analysis



Address: Nussallee 14-16, D-53115 Bonn Fax: (+49) 228 / 73-2505

Data Base

Meson Spectroscopy

Baryon Spectroscopy

NN-interaction

Formalism

Analysis of Other Groups

- [SAID](#)
- [MAID](#)
- [Giessen Uni](#)

BG PWA

- [Publications](#)
- [Talks](#)
- [Contacts](#)

Useful Links

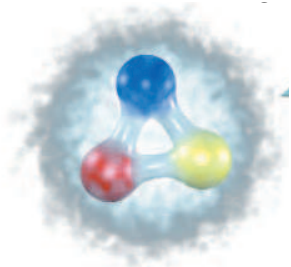
- [SPIRES](#)
- [PDG Homepage](#)
- [Durham Data Base](#)
- [Bonn Homepage](#)

[CB-ELSA Homepage](#)

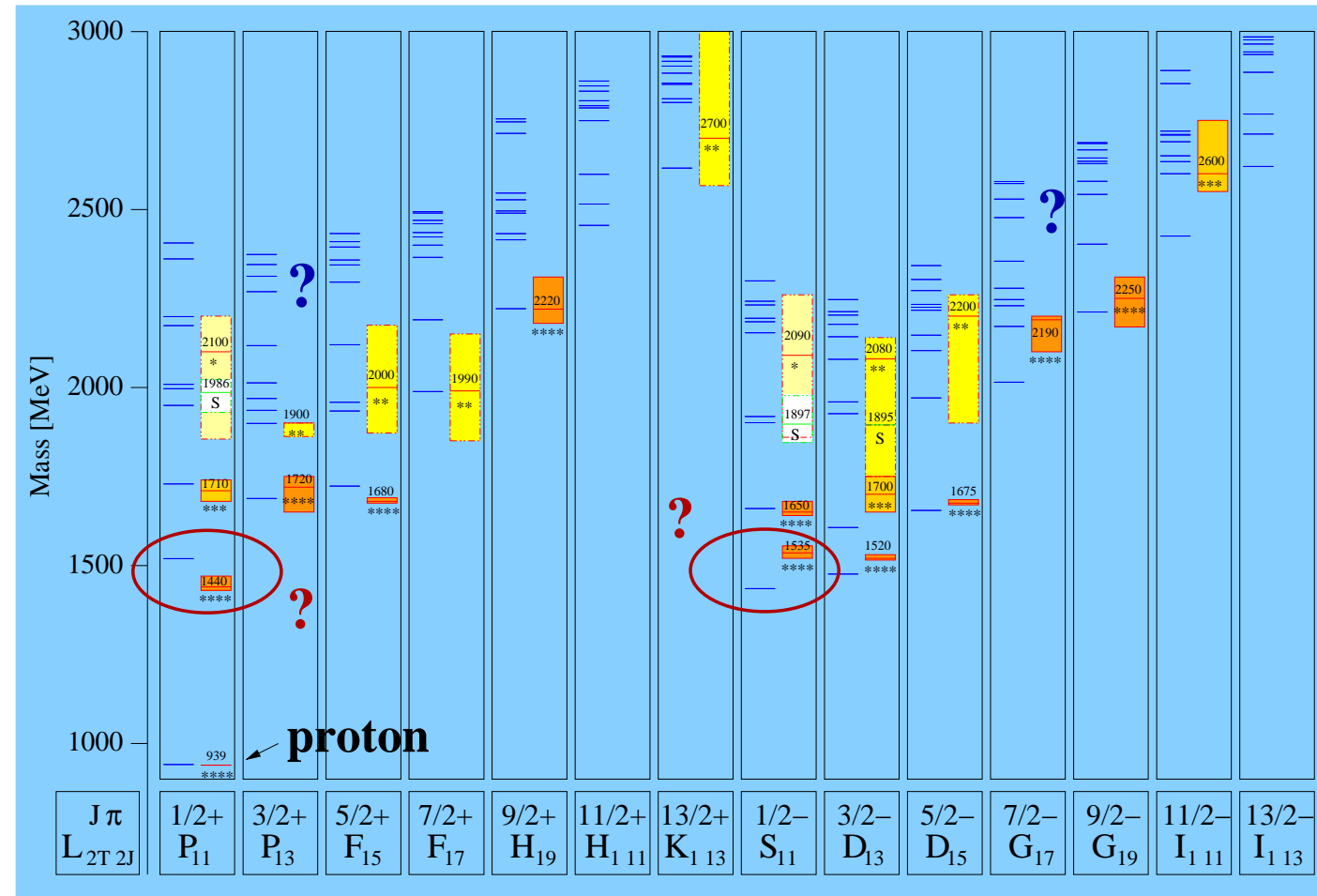
Responsible: Dr. V. Nikonov, E-mail: nikonov@hiskp.uni-bonn.de
Last changes: January 26th, 2010.

N^{*}- resonances in the quark model

Nukleon

 10^{-15} m 

U. Loering, B. Metsch, H. Petry et al. (Bonn)



↔

Constituent
quarks

Confinement-
potential

Residual
interaction

Problems in the baryon spectroscopy and/or quark model:

1. **Problem:** Number of predicted three quark states exceeds dramatically the number of discovered baryons.
2. **Possible solution:** Most of the information comes from analyses of πN elastic reactions. Photoproduction data taken by CLAS, GRAAL, LEPS and CB-ELSA can provide an important information about missing states.
 - (a) **problem:** Unambiguous analysis of photoproduction reactions can not be done without polarization information available.
 - (b) **problem:** Signals in simple reactions are expected to be mostly weak. Strong signals from new resonances can be found in multi-meson final states.
 - (c) **Possible solution 1:** Single polarization observables are measured now by almost all collaborations. Double polarization data are available from CLAS, GRAAL and, in nearest future, from CB-ELSA.
 - (d) **Possible solution 2:** A combined analysis of large data sets.

The latest analysis of SAID (GWU) of πN elastic data as well as $\gamma p \rightarrow \pi^0 p$ and $\gamma p \rightarrow \pi^+ n$ did not confirm the set of states observed in earlier analysis of πN elastic data. CLAS (M. Dugger et al.). Phys.Rev.C79:065206,2009.

State	PDG (Pole position)(MeV)		Bonn-Gatchina PWA (MeV)	
	Mass	Width	Mass	Width
$P_{11}(1710)^{***}$	1720 ± 50	230 ± 150	1710 ± 25	220 ± 20
$P_{33}(1600)^{***}$	1550 ± 100	300 ± 100	1480 ± 40	230 ± 40
$P_{33}(1920)^{***}$	1900 ± 50	200^{+100}_{-50}	1920 ± 50	330 ± 50
$D_{13}(1720)^{***}$	1680 ± 50	100 ± 50	1730 ± 30	170 ± 35
$P_{13}(1900)^{*}$	~ 1900	498 ± 78	1920 ± 30	200 ± 30
$D_{33}(1940)^{*}$	~ 1940	$200 - 500$	1990 ± 40	350 ± 50

Data Base

Pion induced reactions (χ^2 analysis).

Observable	N_{data}	$\frac{\chi^2}{N_{\text{data}}}$		Observable	N_{data}	$\frac{\chi^2}{N_{\text{data}}}$	
$N_{1/2}^*$ S ₁₁ ($\pi N \rightarrow \pi N$)	104	1.81	SAID	$\Delta_{1/2}^-$ S ₃₁ ($\pi N \rightarrow \pi N$)	112	2.27	SAID
$N_{1/2}^*$ P ₁₁ ($\pi N \rightarrow \pi N$)	112	2.49	SAID	$\Delta_{1/2}^+$ P ₃₁ ($\pi N \rightarrow \pi N$)	104	2.01	SAID
$N_{3/2}^*$ P ₁₃ ($\pi N \rightarrow \pi N$)	112	1.90	SAID	$\Delta_{3/2}^*$ P ₃₃ ($\pi N \rightarrow \pi N$)	120	2.53	SAID
$\Delta_{3/2}^*$ D ₃₃ ($\pi N \rightarrow \pi N$)	108	2.56	SAID	$N_{3/2}^*$ D ₁₃ ($\pi N \rightarrow \pi N$)	96	2.16	SAID
$N_{5/2}^*$ D ₁₅ ($\pi N \rightarrow \pi N$)	96	3.37	SAID	$\Delta_{5/2}^+$ F ₃₅ ($\pi N \rightarrow \pi N$)	62	1.32	SAID
$\Delta_{7/2}^+$ F ₃₇ ($\pi N \rightarrow \pi N$)	72	2.86	SAID				
$d\sigma/d\Omega(\pi^- p \rightarrow n\eta)$	70	1.96	Richards <i>et al.</i>	$d\sigma/d\Omega(\pi^- p \rightarrow n\eta)$	84	2.67	CBALL
$d\sigma/d\Omega(\pi^- p \rightarrow K\Lambda)$	598	1.68	RAL	$P(\pi^- p \rightarrow K\Lambda)$	355	1.96	RAL+ANL
$d\sigma/d\Omega(\pi^+ p \rightarrow K^+\Sigma)$	609	1.24	RAL	$P(\pi^+ p \rightarrow K^+\Sigma)$	307	1.49	RAL
$d\sigma/d\Omega(\pi^- p \rightarrow K^0\Sigma^0)$	259	0.85	RAL	$P(\pi^- p \rightarrow K^0\Sigma^0)$	95	1.25	RAL

Data Base

π and η photoproduction reactions (χ^2 analysis).

Observable	N_{data}	$\frac{\chi^2}{N_{\text{data}}}$		Observable	N_{data}	$\frac{\chi^2}{N_{\text{data}}}$	
$d\sigma/d\Omega(\gamma p \rightarrow p\pi^0)$	1106	1.34	CB-ELSA	$d\sigma/d\Omega(\gamma p \rightarrow p\pi^0)$	861	1.46	GRAAL
$d\sigma/d\Omega(\gamma p \rightarrow p\pi^0)$	592	2.11	CLAS	$d\sigma/d\Omega(\gamma p \rightarrow p\pi^0)$	1692	1.25	TAPS@MAMI
$E(\gamma p \rightarrow p\pi^0)$	140	1.23	A2-GDH	$\Sigma(\gamma p \rightarrow p\pi^0)$	1492	3.26	SAID db
$P(\gamma p \rightarrow p\pi^0)$	607	3.23	SAID db	$T(\gamma p \rightarrow p\pi^0)$	389	3.71	SAID db
$H(\gamma p \rightarrow p\pi^0)$	71	1.26	SAID db	$G(\gamma p \rightarrow p\pi^0)$	75	1.50	SAID db
$O_x(\gamma p \rightarrow p\pi^0)$	7	1.77	SAID db	$O_z(\gamma p \rightarrow p\pi^0)$	7	0.46	SAID db
$d\sigma/d\Omega(\gamma p \rightarrow n\pi^+)$	1583	1.64	SAID db	$d\sigma/d\Omega(\gamma p \rightarrow n\pi^+)$	408	0.62	A2-GDH
$\Sigma(\gamma p \rightarrow n\pi^+)$	899	3.48	SAID db	$E(\gamma p \rightarrow n\pi^+)$	231	1.55	A2-GDH
$P(\gamma p \rightarrow n\pi^+)$	252	2.90	SAID db	$T(\gamma p \rightarrow n\pi^+)$	661	3.21	SAID db
$H(\gamma p \rightarrow p\pi^+)$	71	3.90	SAID db	$G(\gamma p \rightarrow p\pi^+)$	86	5.64	SAID db
$d\sigma/d\Omega(\gamma p \rightarrow p\eta)$	680	1.47	CB-ELSA	$d\sigma/d\Omega(\gamma p \rightarrow p\eta)$	100	2.16	TAPS
$\Sigma(\gamma p \rightarrow p\eta)$	51	2.26	GRAAL 98	$\Sigma(\gamma p \rightarrow p\eta)$	100	2.02	GRAAL 07
$T(\gamma p \rightarrow p\eta)$	50	1.48	Phoenics				

Data Base

Kaon photoproduction (χ^2 analysis).

Observable	N_{data}	$\frac{\chi^2}{N_{\text{data}}}$		Observable	N_{data}	$\frac{\chi^2}{N_{\text{data}}}$	
$C_x(\gamma p \rightarrow \Lambda K^+)$	160	1.23	CLAS	$C_x(\gamma p \rightarrow \Sigma^0 K^+)$	94	2.20	CLAS
$C_z(\gamma p \rightarrow \Lambda K^+)$	160	1.41	CLAS	$C_z(\gamma p \rightarrow \Sigma^0 K^+)$	94	2.00	CLAS
$d\sigma/d\Omega(\gamma p \rightarrow \Lambda K^+)$	1320	0.81	CLAS09	$d\sigma/d\Omega(\gamma p \rightarrow \Sigma^0 K^+)$	1280	2.06	CLAS
$P(\gamma p \rightarrow \Lambda K^+)$	1270	2.21	CLAS09	$P(\gamma p \rightarrow \Sigma^0 K^+)$	95	1.45	CLAS
$\Sigma(\gamma p \rightarrow \Lambda K^+)$	66	1.53	GRAAL	$\Sigma(\gamma p \rightarrow \Sigma^0 K^+)$	42	0.90	GRAAL
$\Sigma(\gamma p \rightarrow \Lambda K^+)$	45	1.65	LEP	$\Sigma(\gamma p \rightarrow \Sigma^0 K^+)$	45	1.11	LEP
$T(\gamma p \rightarrow \Lambda K^+)$	66	1.26	GRAAL 09	$d\sigma/d\Omega(\gamma p \rightarrow \Sigma^+ K^0)$	48	3.76	CLAS
$O_x(\gamma p \rightarrow \Lambda K^+)$	66	1.30	GRAAL 09	$O_z(\gamma p \rightarrow \Lambda K^+)$	66	1.54	GRAAL 09
$d\sigma/d\Omega(\gamma p \rightarrow \Sigma^+ K^0)$	72	0.74	CB-ELSA 10	$P(\gamma p \rightarrow \Sigma^+ K^0)$	24	1.06	CB-ELSA 10
$\Sigma(\gamma p \rightarrow \Sigma^+ K^0)$	15	1.13	CB-ELSA 10				

Data Base

Multi-meson final states (maximum likelihood analysis).

$d\sigma/d\Omega(\pi^- p \rightarrow n\pi^0\pi^0)$	CBALL					
$d\sigma/d\Omega(\gamma p \rightarrow p\pi^0\pi^0)$	CB-ELSA (1.4 GeV)	$E(\gamma p \rightarrow p\pi^0\pi^0)$	16	1.91	MAMI	
$d\sigma/d\Omega(\gamma p \rightarrow p\pi^0\eta)$	CB-ELSA (3.2 GeV)	$\Sigma(\gamma p \rightarrow p\pi^0\eta)$	180	2.37	GRAAL	
$d\sigma/d\Omega(\gamma p \rightarrow p\pi^0\pi^0)$	CB-ELSA (3.2 GeV)	$\Sigma(\gamma p \rightarrow p\pi^0\pi^0)$	128	0.96	GRAAL	
$d\sigma/d\Omega(\gamma p \rightarrow p\pi^0\eta)$	CB-ELSA (3.2 GeV)	$\Sigma(\gamma p \rightarrow p\pi^0\eta)$	180	2.37	GRAAL	
$I_c(\gamma p \rightarrow p\pi^0\eta)$	CB-ELSA (3.2 GeV)	$I_s(\gamma p \rightarrow p\pi^0\eta)$				CB-ELSA (3.2 GeV)

Energy dependent approach

In many cases an unambiguous partial wave decomposition at fixed energies is impossible. Then the energy and angular parts should be analyzed together:

$$A(s, t) = \sum_{\beta\beta'n} A_n^{\beta\beta'}(s) Q_{\mu_1 \dots \mu_n}^{(\beta)} F_{\nu_1 \dots \nu_n}^{\mu_1 \dots \mu_n} Q_{\nu_1 \dots \nu_n}^{(\beta')}$$

1. C. Zemach, Phys. Rev. 140, B97 (1965); 140, B109 (1965).
 2. S.U.Chung, Phys. Rev. D 57, 431 (1998).
 3. A.V. Anisovich *et al.* J. Phys. G 28 15 (2002)
V. V. Anisovich, M. A. Matveev, V. A. Nikonov, J. Nyiri and A. V. Sarantsev,
Hackensack, USA: World Scientific (2008) 580 p
1. Correlations between angular part and energy part are under control.
 2. Unitarity and analyticity can be introduced from the beginning.
 3. However, to fix simultaneously energy and angular dependencies of the amplitude a combined fit of many reactions is needed.

Combined analysis of pion- and photo-production data:

For pion induced reactions:

$$A_{1i} = K_{1j}(I - i\rho K)_{ji}^{-1}$$

and

$$K_{ij} = \sum_{\alpha} \frac{g_i^{\alpha} g_j^{\alpha}}{M_{\alpha}^2 - s} + f_{ij}(s) \quad f_{ij} = \frac{f_{ij}^{(1)} + f_{ij}^{(2)} \sqrt{s}}{s - s_0^{ij}}.$$

where f_{ij} is nonresonant transition part.

For the photoproduction:

$$A_k = P_j(I - i\rho K)_{jk}^{-1}$$

The vector of the initial interaction has the form:

$$P_j = \sum_{\alpha} \frac{\Lambda^{\alpha} g_j^{\alpha}}{M_{\alpha}^2 - s} + F_j(s)$$

Here F_j is nonresonant production of the final state j .

Bonn-Gatchina partial wave analysis

1. **K-matrix:** $\pi N \rightarrow \pi N, \pi N \rightarrow \eta N, \pi N \rightarrow K\Lambda$ and $\pi N \rightarrow K\Sigma$ reactions.

Included channels: $\pi N, \eta N, K\Lambda, K\Sigma, \pi\Delta(1232), N\sigma, N\rho$.

First results for the S_{11} wave fitted in the N/D approach.

2. **P-vector:** $\gamma N \rightarrow \pi N, \gamma N \rightarrow \eta N, \gamma N \rightarrow K\Lambda$ and $\gamma N \rightarrow K\Sigma$ reactions.

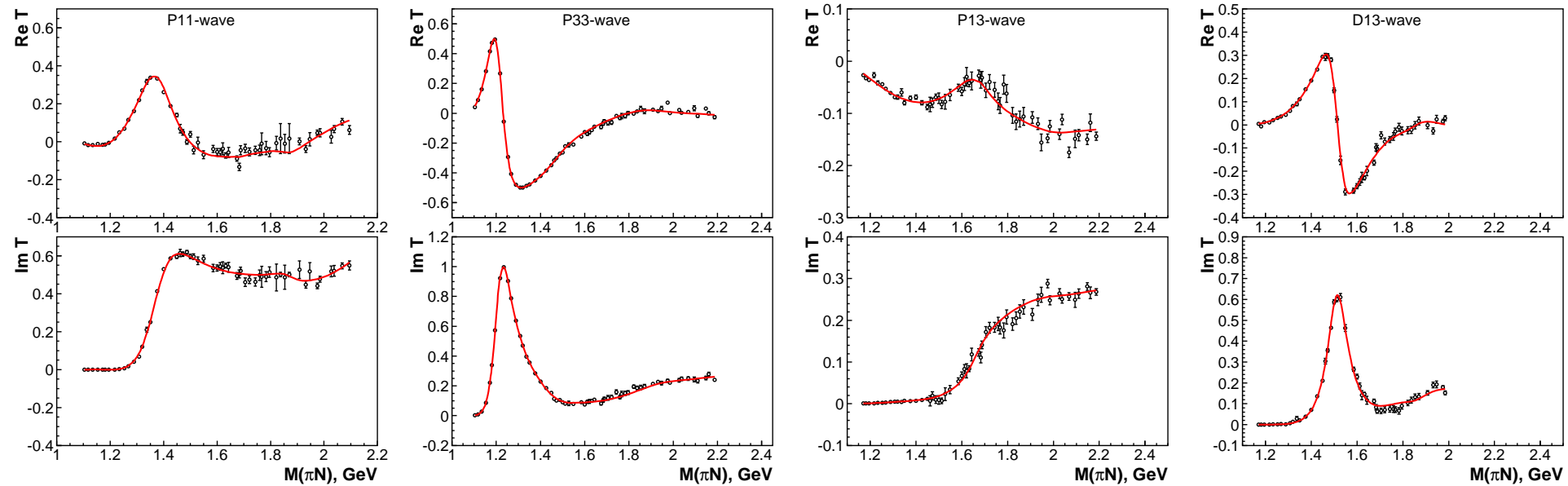
Preliminary fit with Regge exchanges included in the P -vectors.

3. **D-vector:** $\pi N \rightarrow \pi\pi N$

4. **PD-approach** $\gamma N \rightarrow \pi\pi N, \gamma N \rightarrow \pi\eta N$

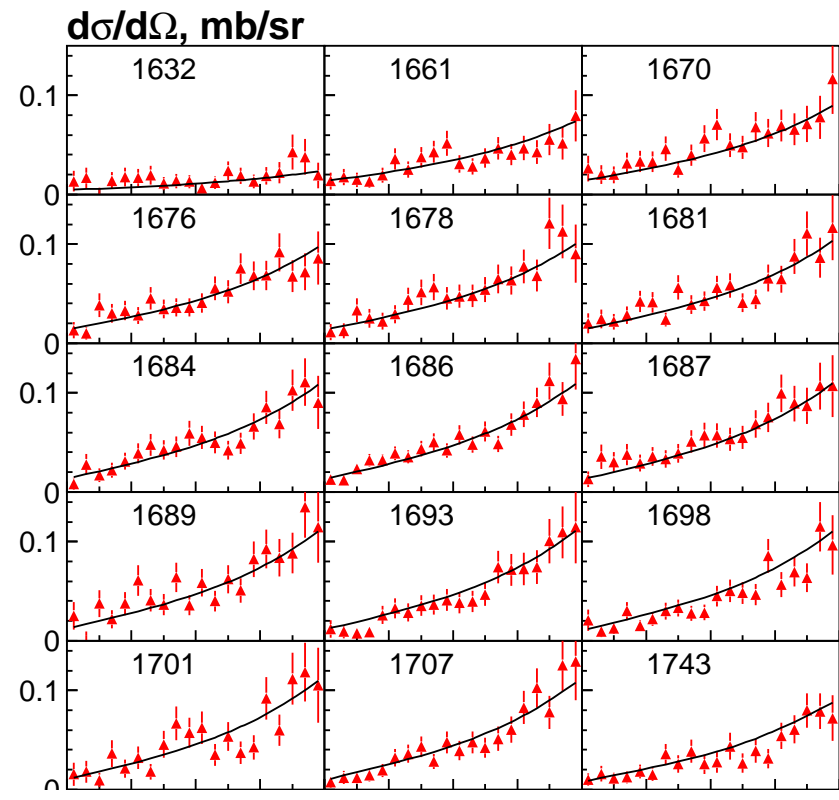
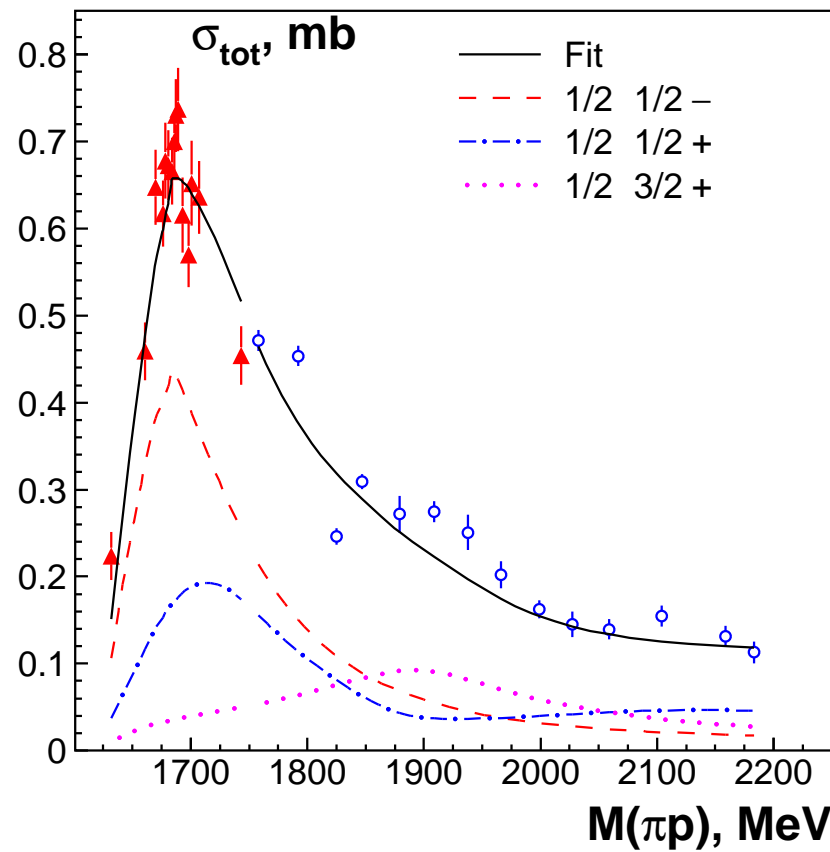
D-vector channels: $P_{11}(1440)\pi, D_{13}(1520)\pi, F_{15}(1675)\pi, f_2(1275)N, \Delta\eta, \dots$

Fit of the SAID energy fixed solution for πN elastic partial waves

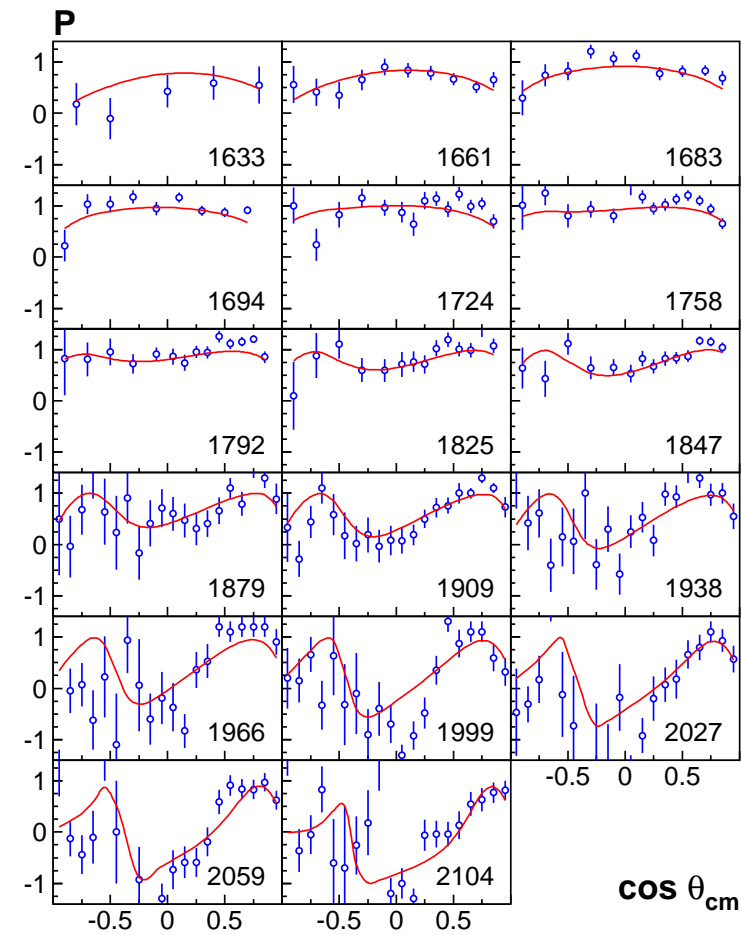
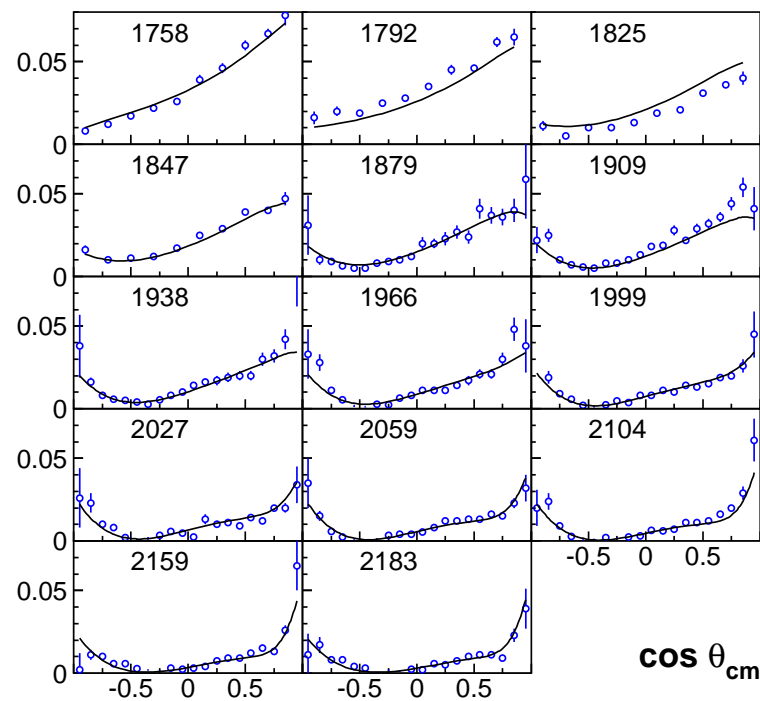


The fit of the the $\pi^- p \rightarrow K\Lambda$ reaction

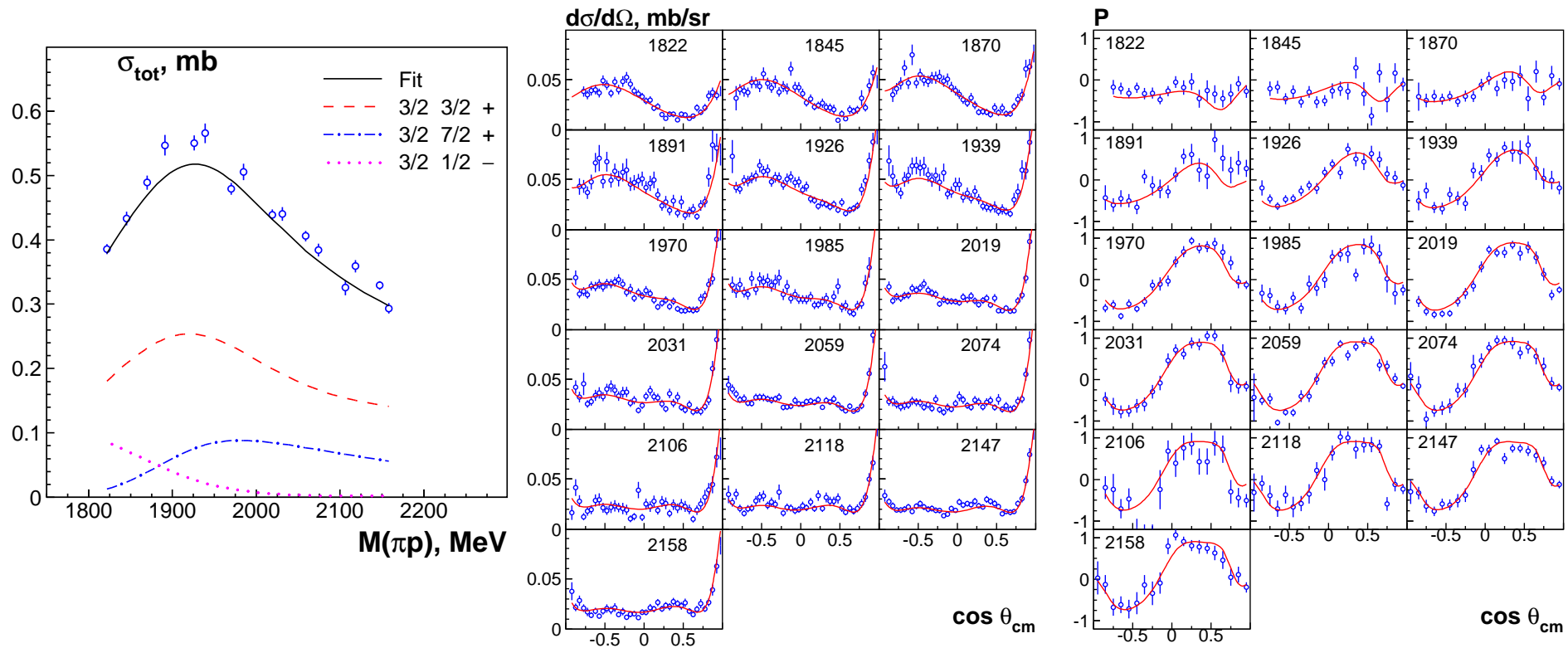
The $P_{11}(1710)$ and $P_{13}(1900)$ states



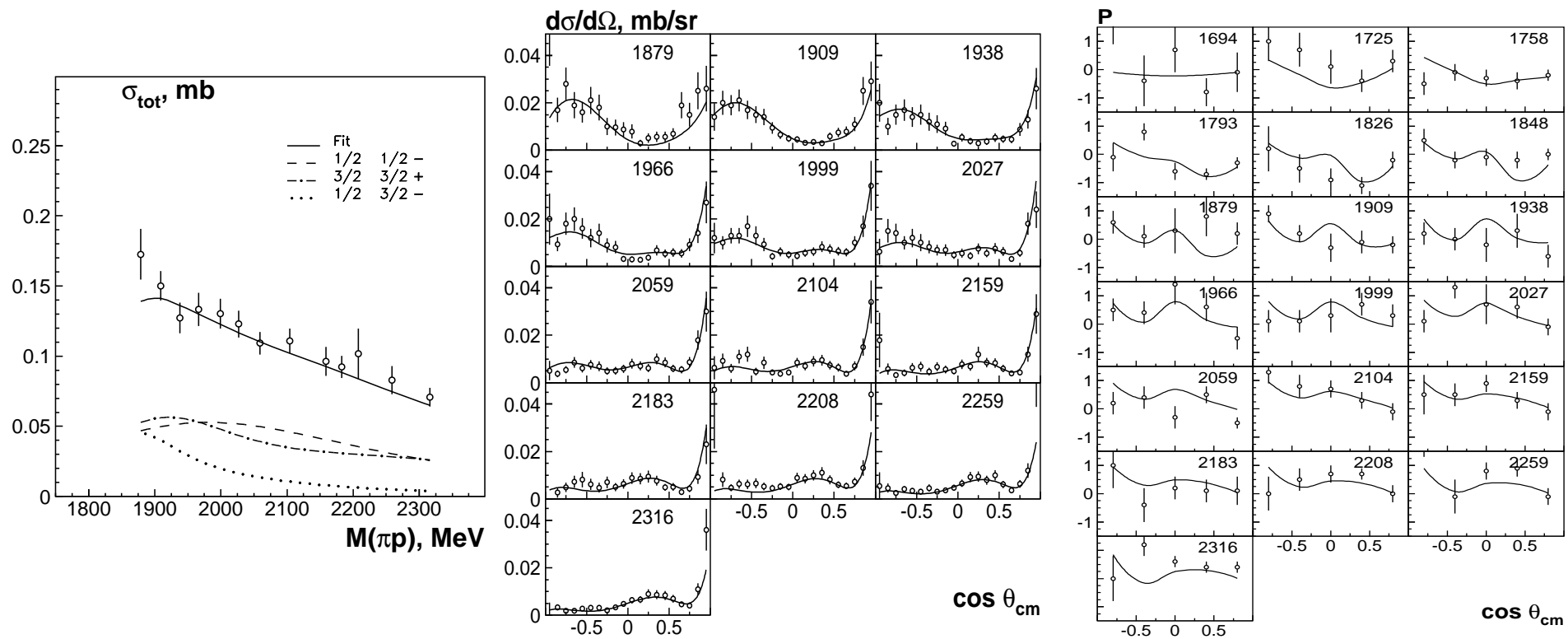
The fit of the the $\pi^- p \rightarrow K\Lambda$ reaction



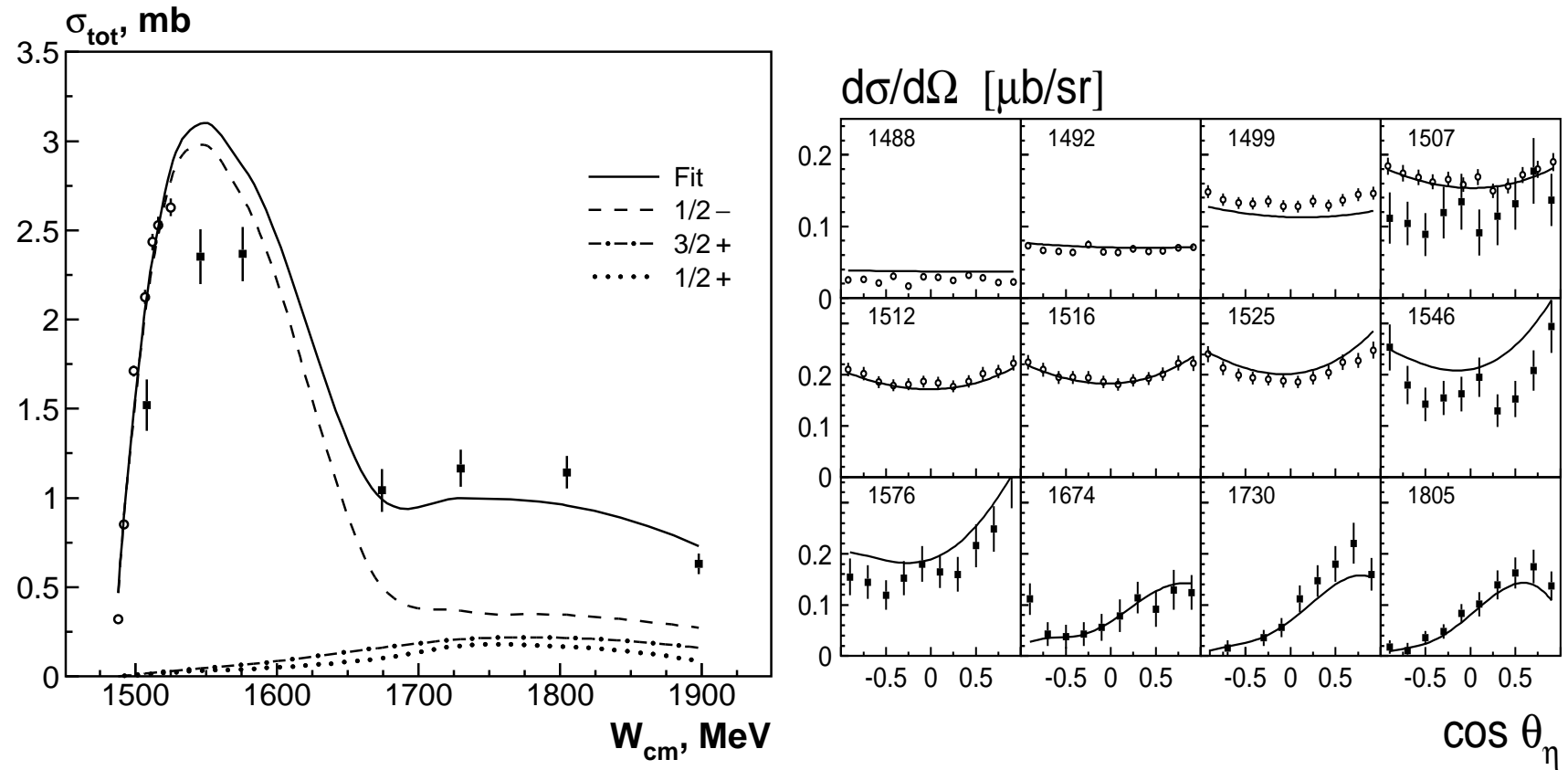
The fit of the the $\pi^+ p \rightarrow K^+ \Sigma^+$ reaction

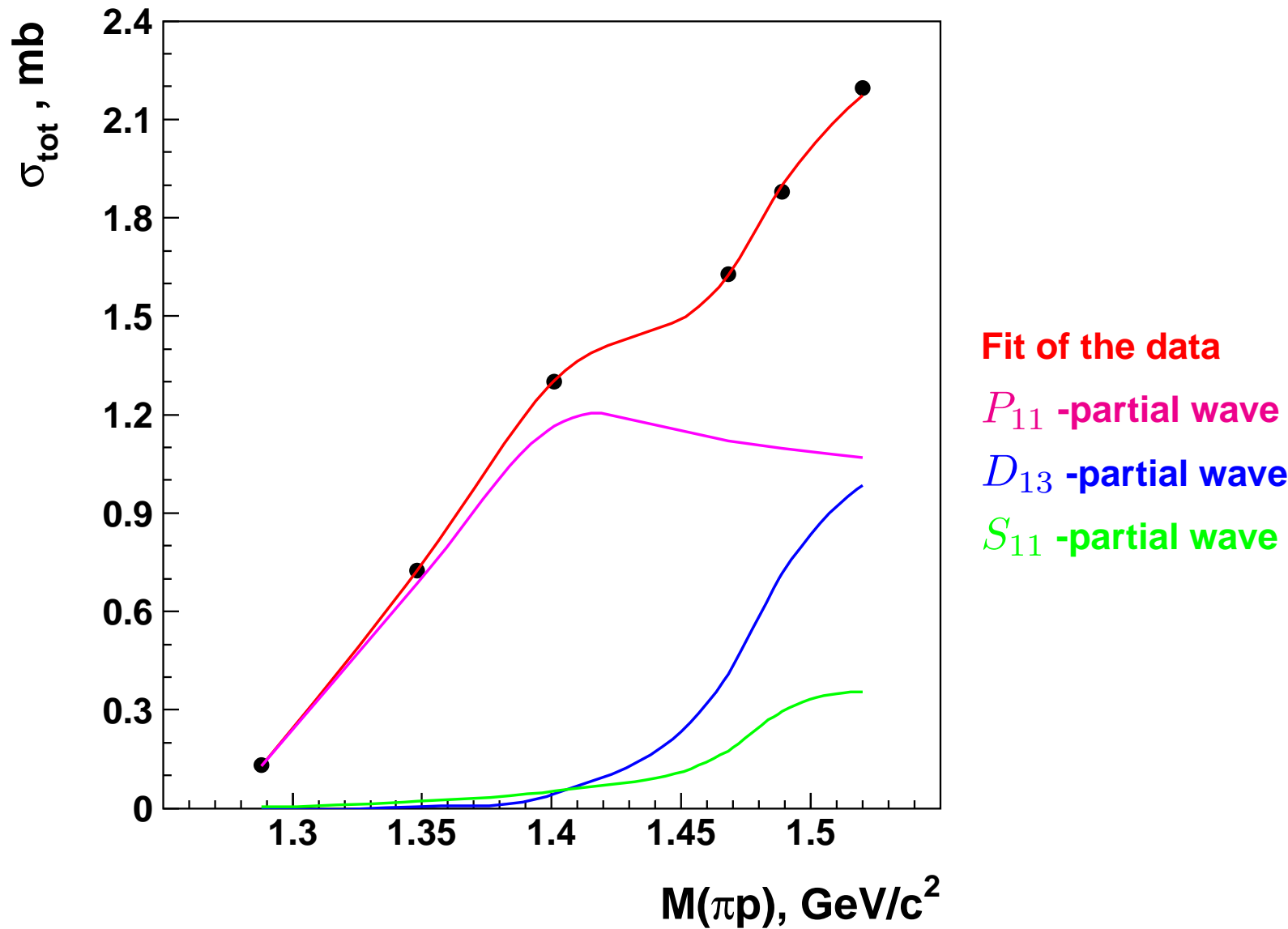


The fit of the the $\pi^- p \rightarrow K^0 \Sigma^0$ reaction



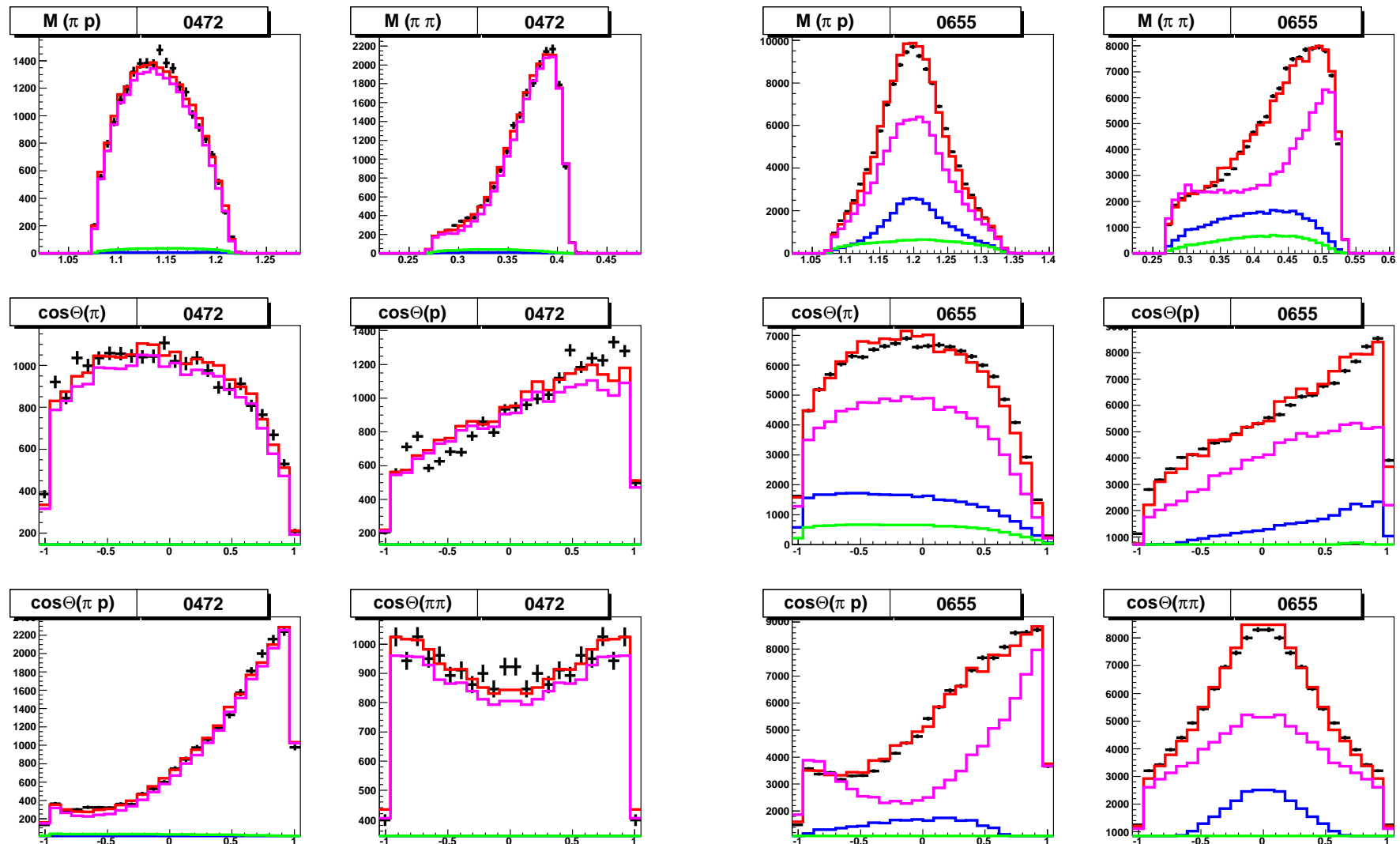
The fit of the $\pi^- p \rightarrow \eta n$ reaction



$\pi^- p \rightarrow n \pi^0 \pi^0$ (Crystal Ball) total cross section

$$\pi^- p \rightarrow n \pi^0 \pi^0$$
 (Crystal Ball)

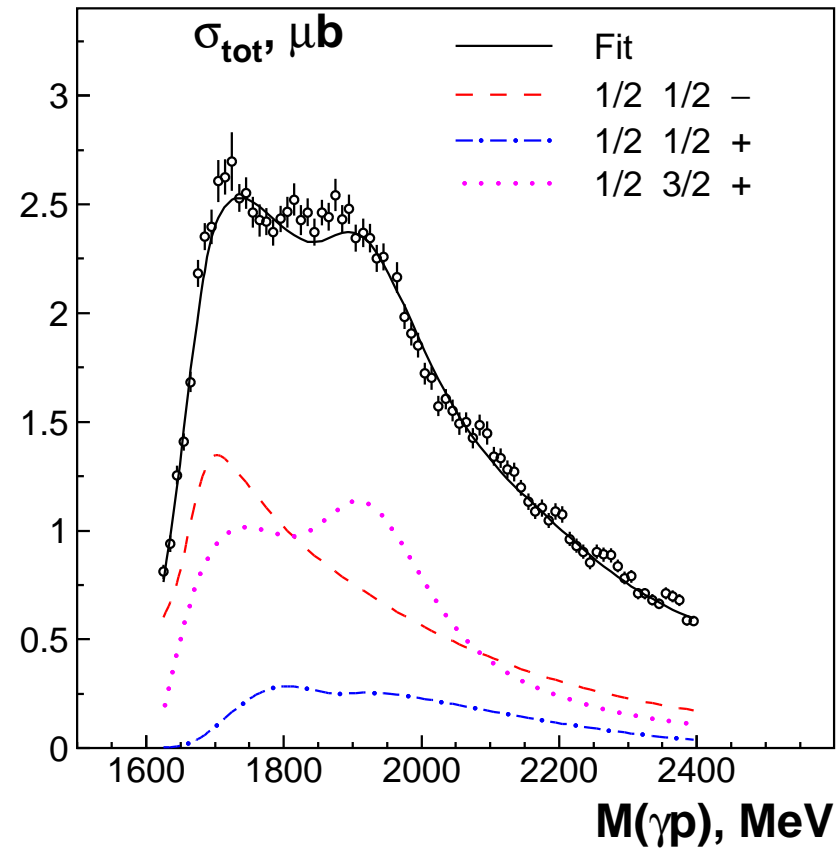
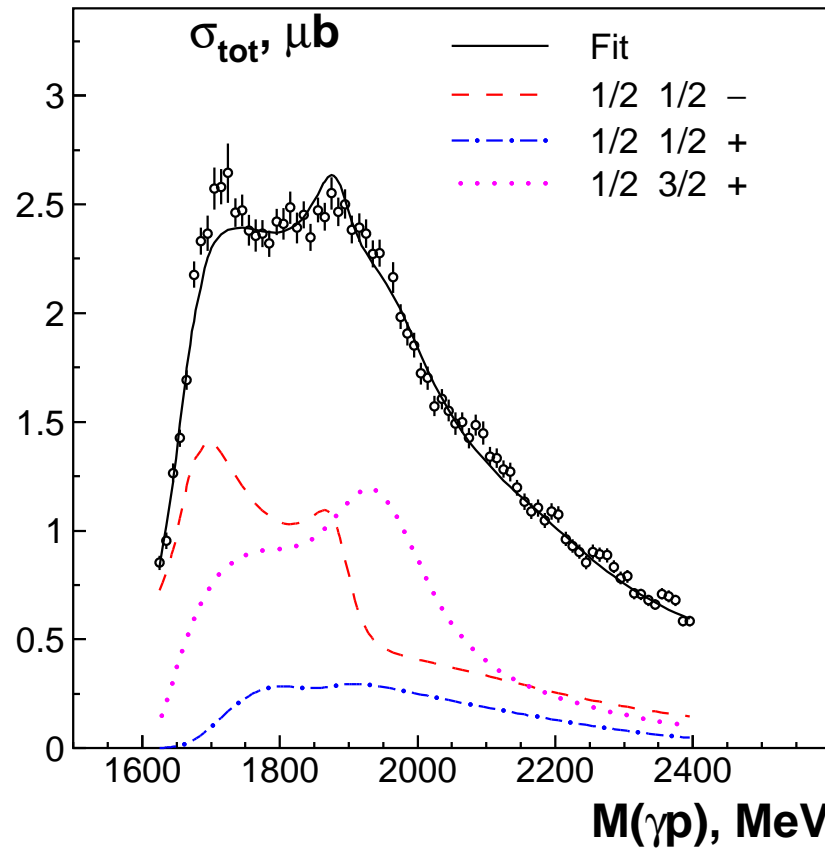
Differential cross sections for 472 and 665 MeV/c data.



Description of all fitted single meson photoproduction observables as well as multipoles can be downloaded in numerical form or as PDF figures from

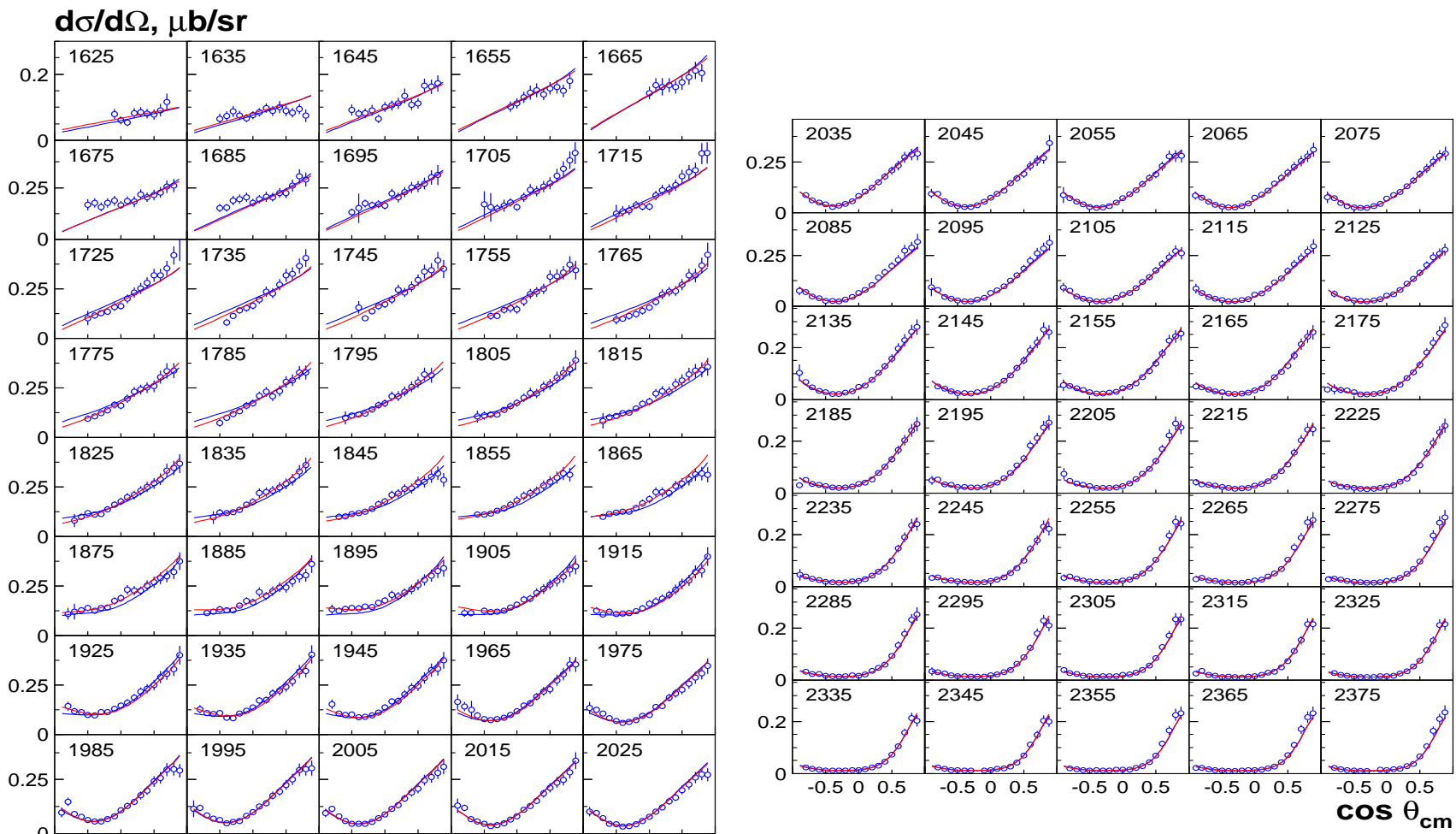
PWA.HISKP.UNI-BONN.DE

The $\gamma p \rightarrow K\Lambda$ reaction (CLAS 2009)



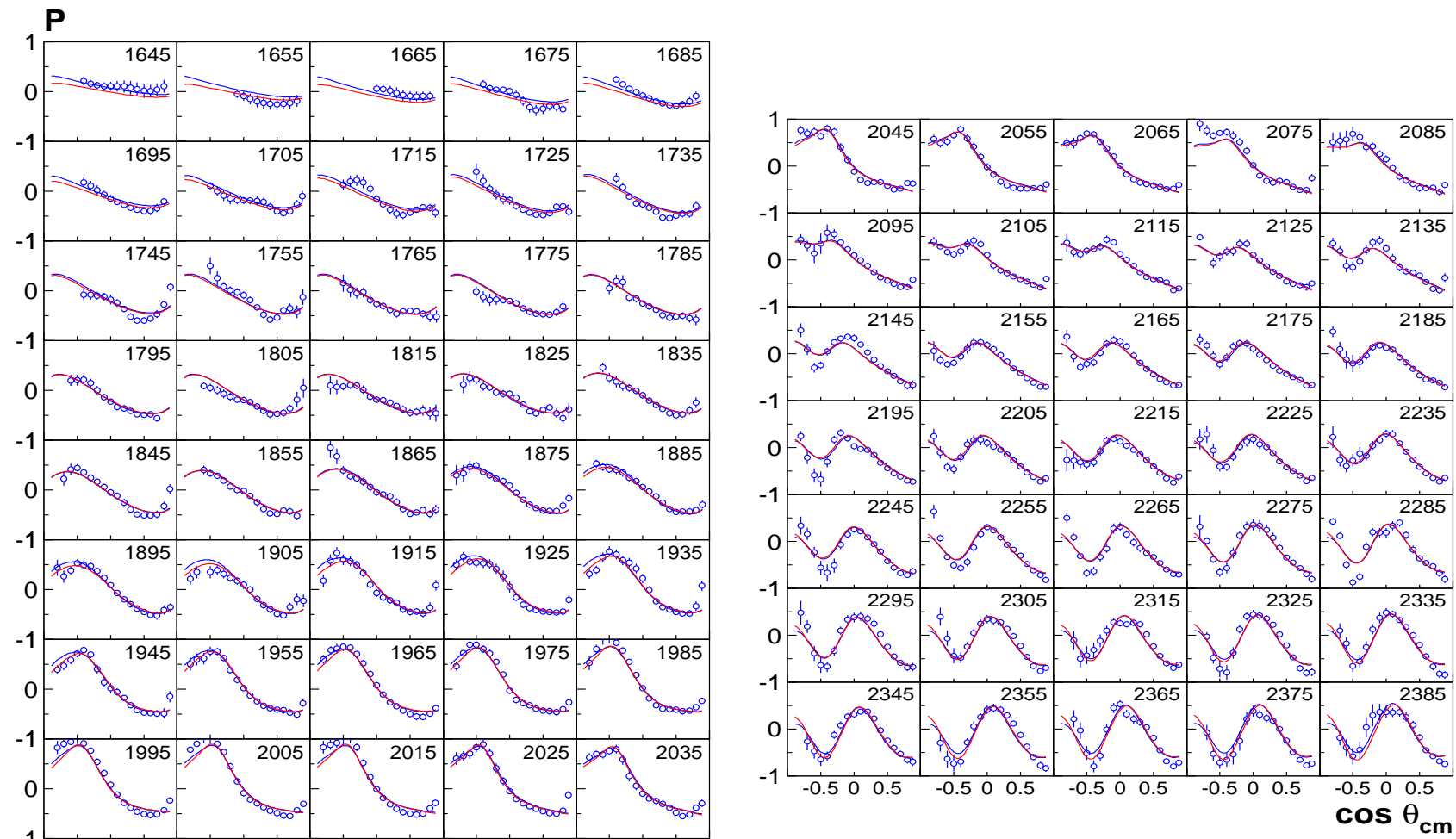
In the first solution the new S_{11} state with mass 1890 ± 10 MeV and width 90 ± 10 MeV is introduced in the fit.

**The fit of the $\gamma p \rightarrow K\Lambda$ differential cross section
(CLAS 2009)**

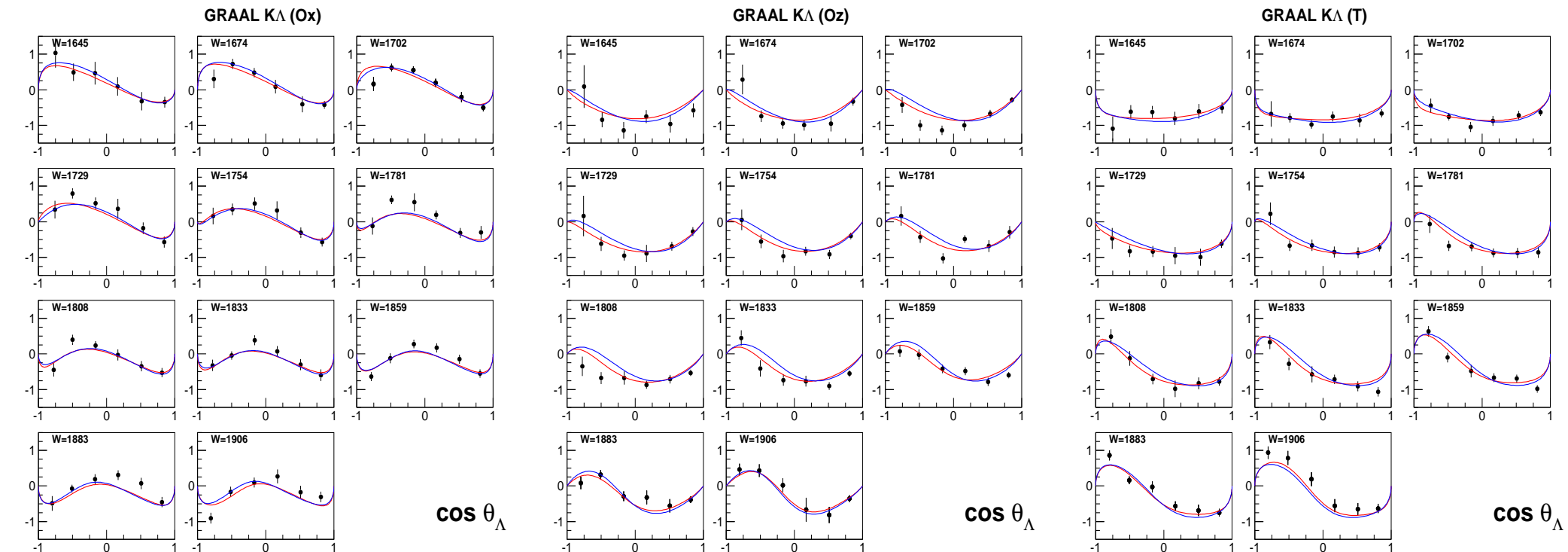


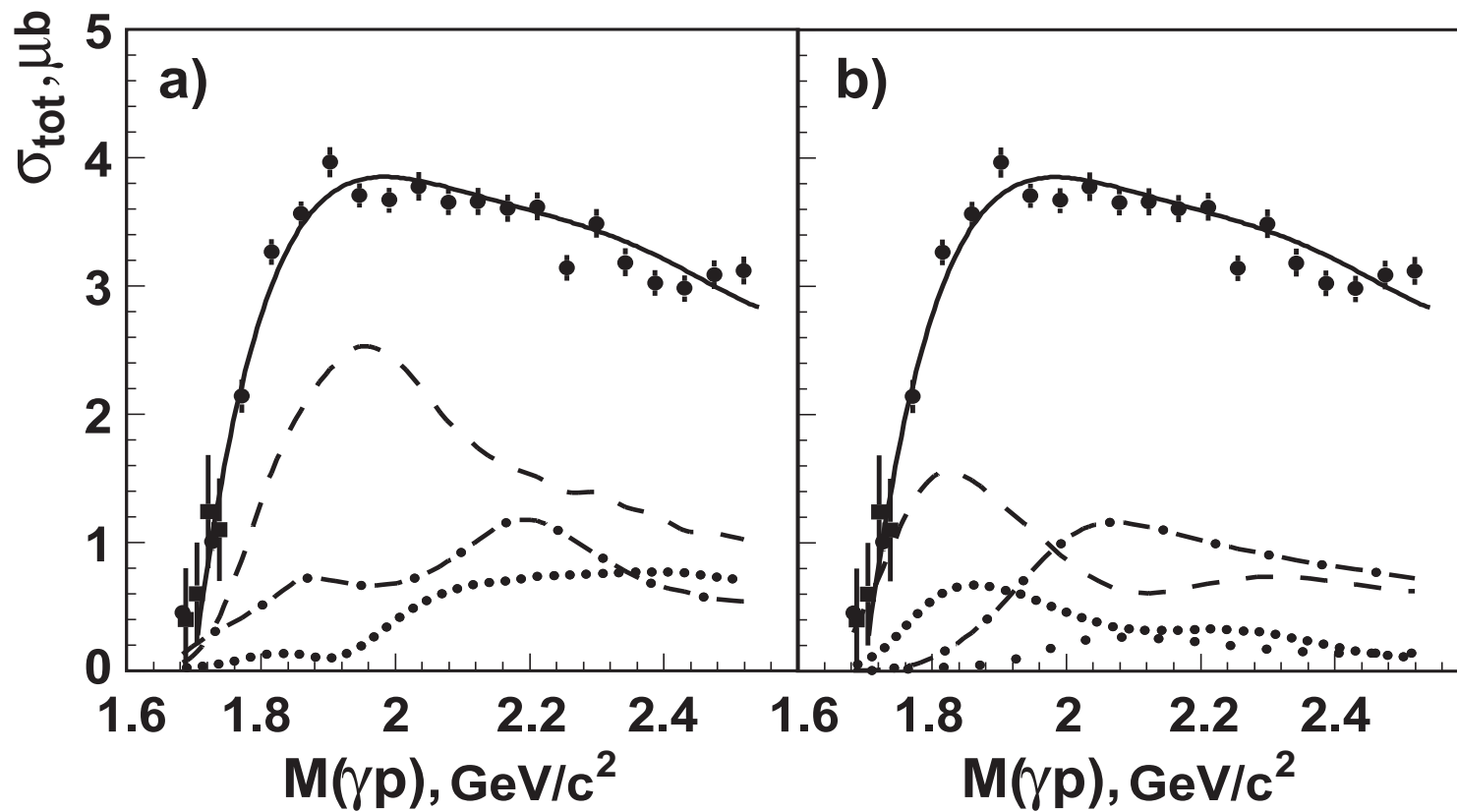
The fit of the $\gamma p \rightarrow K\Lambda$ recoil asymmetry

(CLAS 2009)



The O_x , O_z and T observables from the $\gamma p \rightarrow K\Lambda$ reaction (GRAAL)

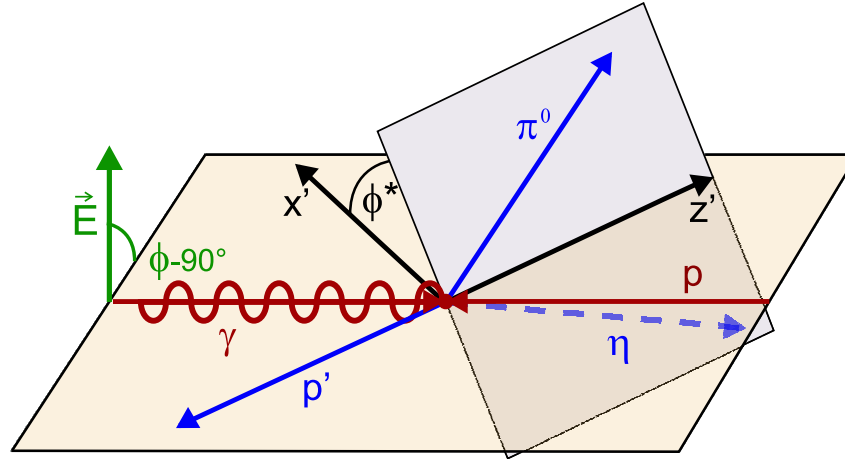


$\gamma p \rightarrow p\pi^0\eta$ (CB-ELSA)


Left panel : contributions from $\Delta(1232)\eta$ (dashed), $S_{11}(1535)\pi$ (dashed-dotted) and $N a_0(980)$ final states.

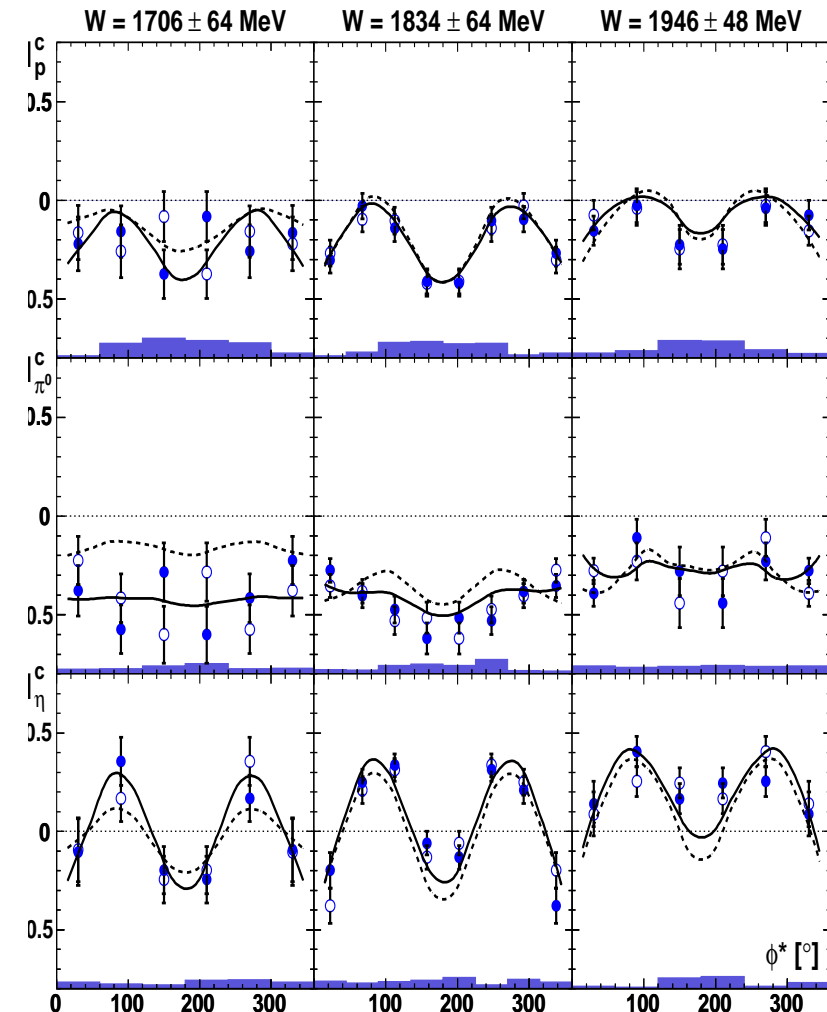
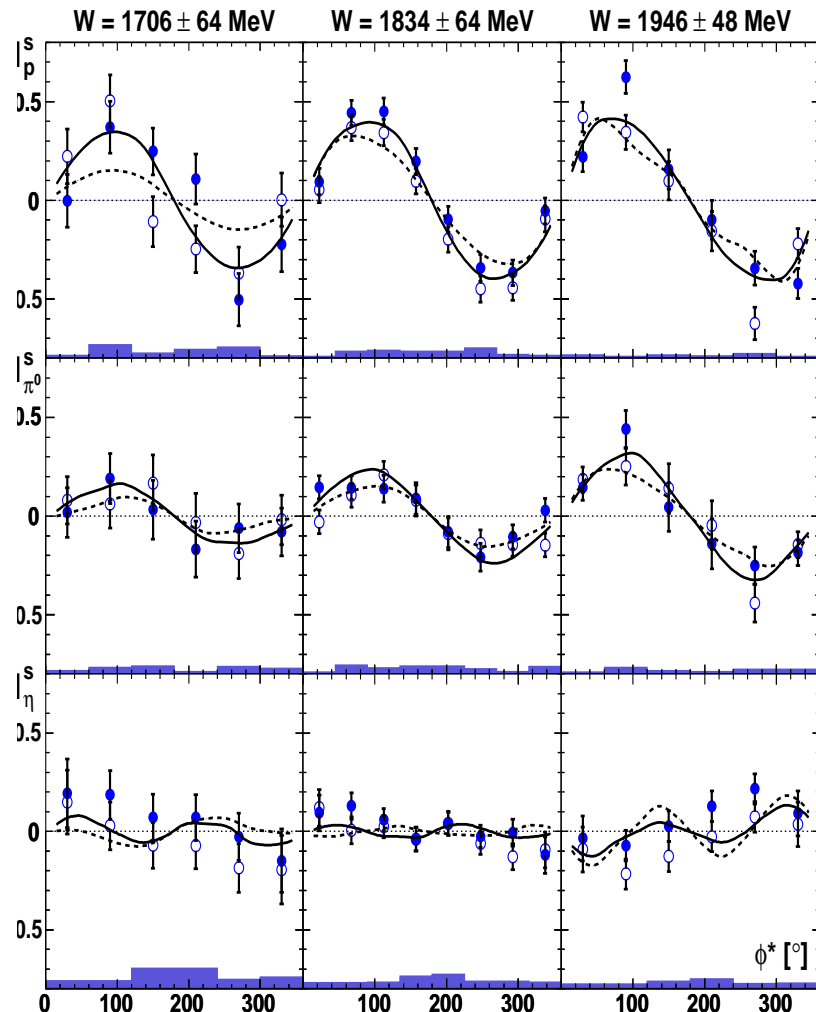
Right panel: D_{33} partial wave (dashed), P_{33} partial wave (dashed-dotted), $D_{33} \rightarrow \Delta(1232)\eta$ (dotted) and $D_{33} \rightarrow N a_0(980)$ (wide dotted).

$\gamma p \rightarrow p\pi^0\eta$ (**CB-ELSA**) with linear polarized photon



$$\frac{d\sigma}{d\Omega} = \left(\frac{d\sigma}{d\Omega} \right)_0 \{ 1 + \delta_l [I^s \sin(2\phi) + I^c \cos(2\phi)] \}, \quad (1)$$

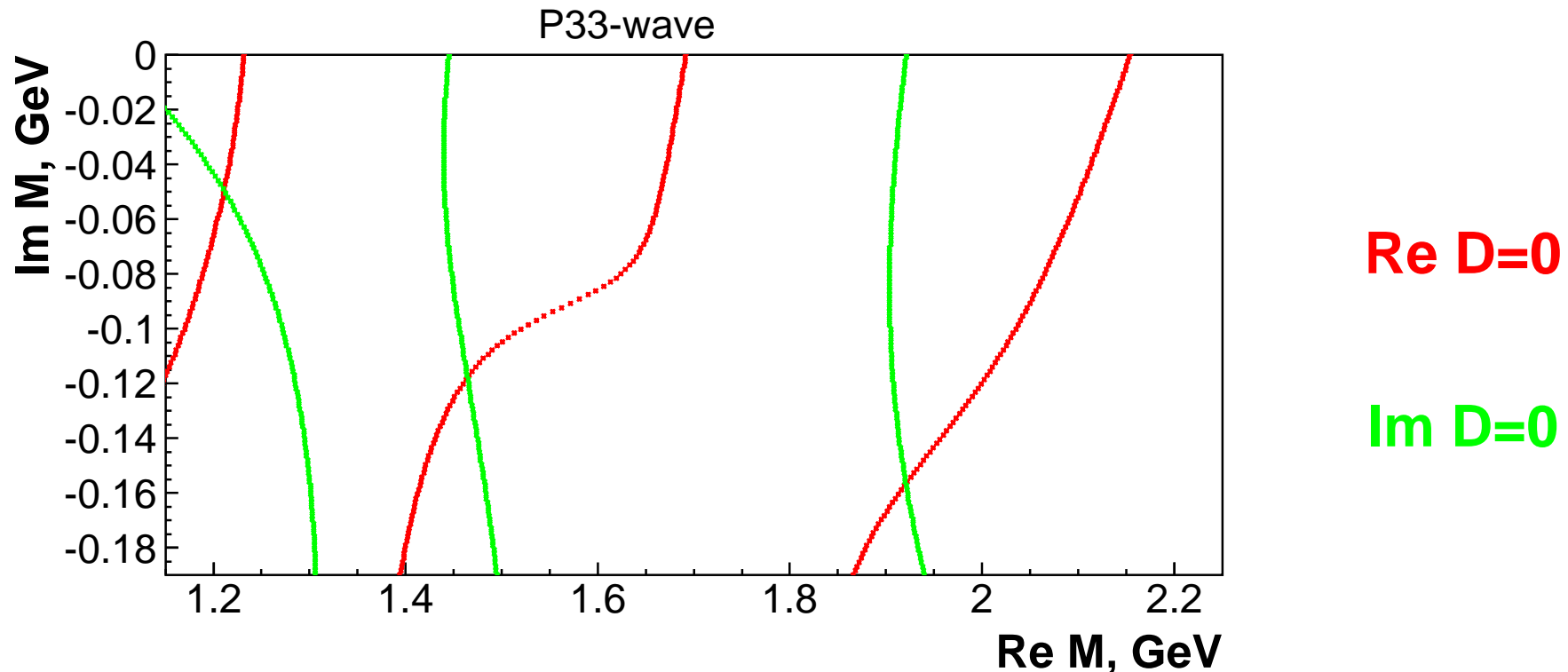
$$\Sigma = \int_0^{2\pi} I^c d\phi^*$$

I^c and I^s for $\gamma p \rightarrow p\pi^0\eta$ (CB-ELSA)


Search for the pole position in the complex plane

P_{33} wave (4 pole 6 channel K-matrix)

$$D = \det(I - i\rho K) \prod_i (M_i^2 - s) \quad \text{1-pole : } D = M^2 - s - i \sum_j \rho_j(s) g_j^2$$

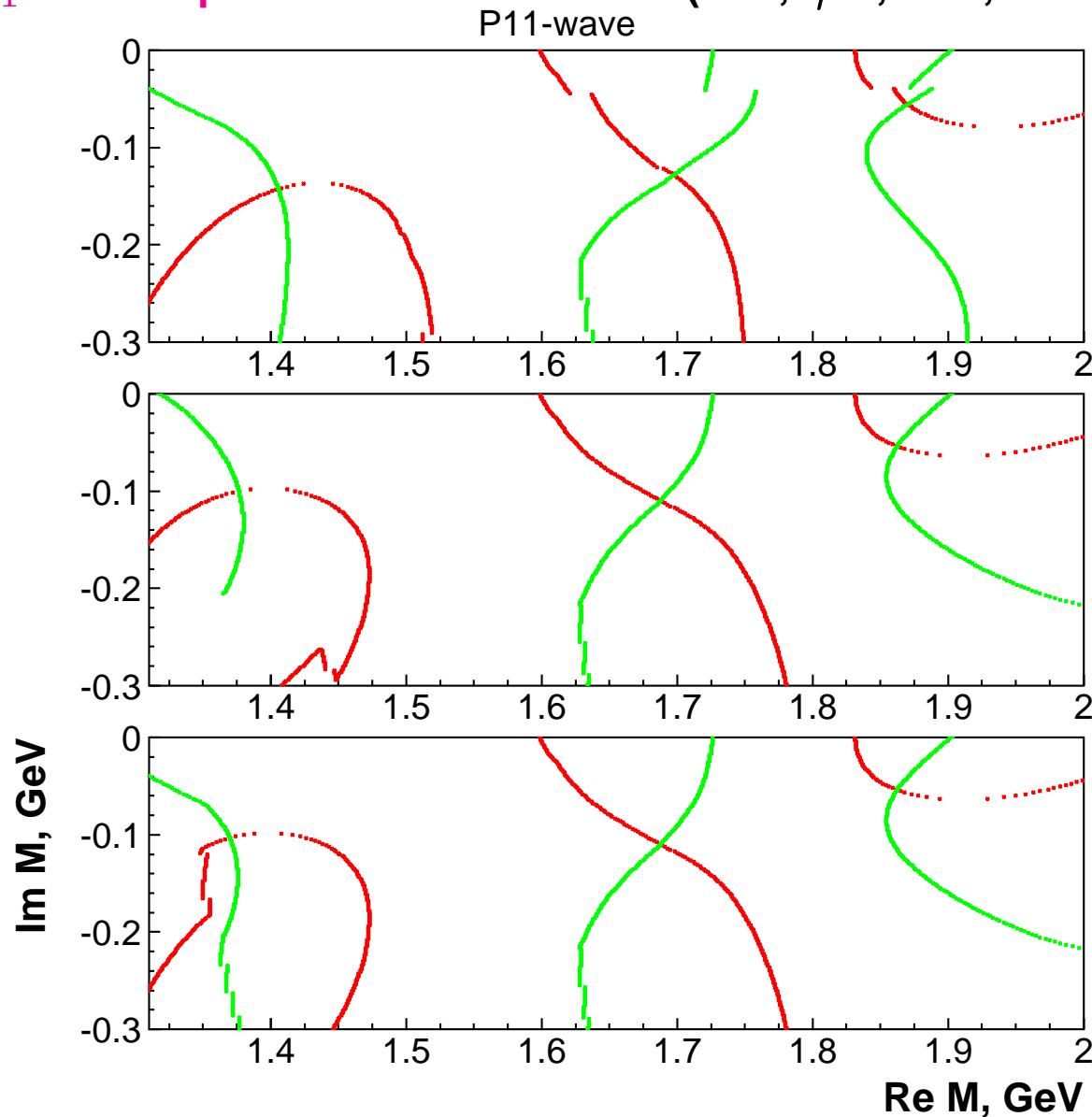


$M = 1210 - i50 \text{ MeV};$

$M = 1485 - i120 \text{ MeV}$

$M = 1920 - i160 \text{ MeV}$

P_{11} wave: 4 pole 6 channel K-matrix ($\pi N, \eta N, K\Lambda, K\Sigma, \pi\Delta(1232), N\sigma$. Solution 1.)



Re $D=0$
Im $D=0$

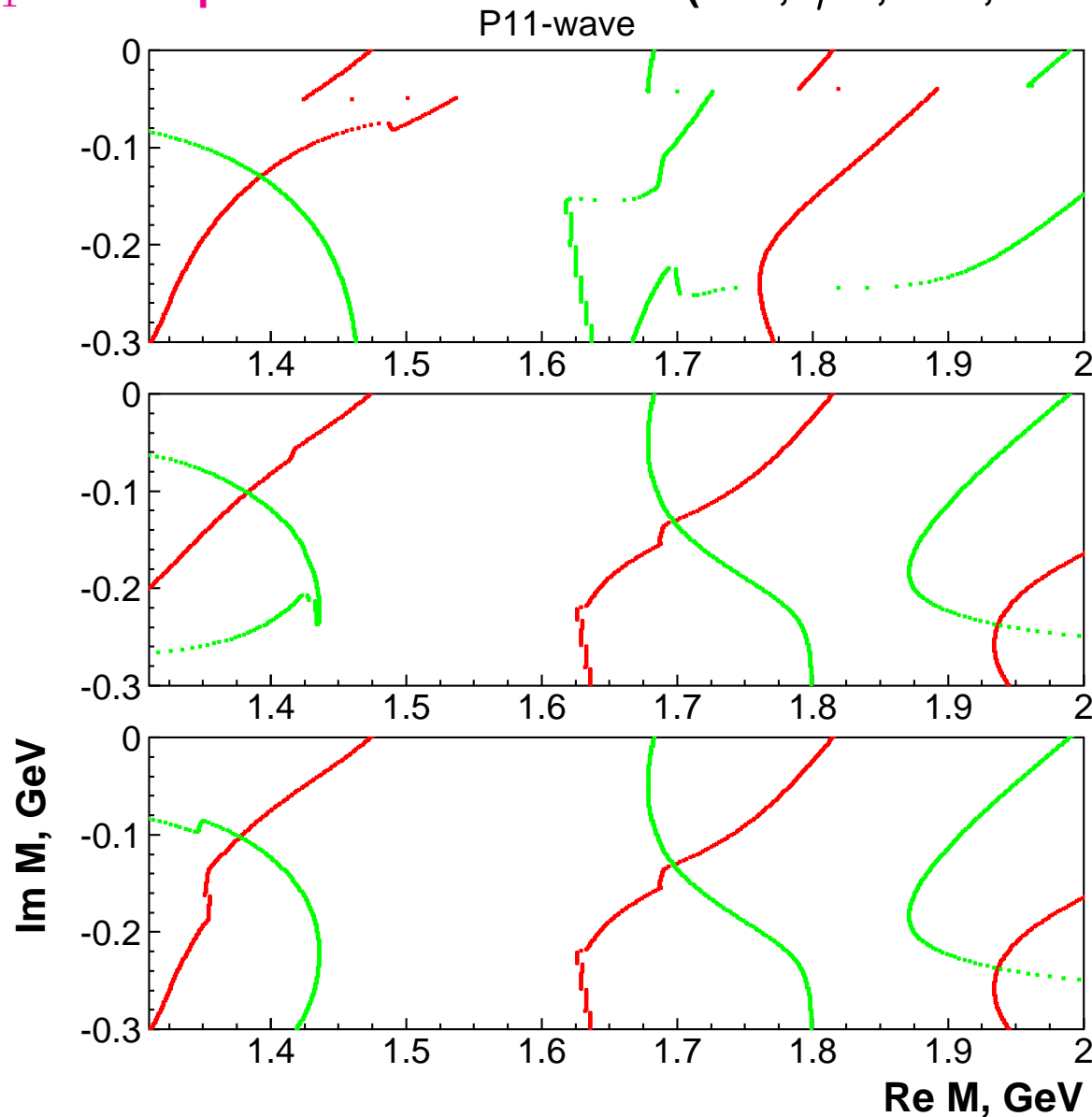
T-matrix poles:

$$M = 1370 - i100 \text{ MeV};$$

$$M = 1695 - i105 \text{ MeV}$$

$$M = 1860 - i60 \text{ MeV}$$

P_{11} wave: 4 pole 6 channel K-matrix ($\pi N, \eta N, K\Lambda, K\Sigma, \pi\Delta(1232), N\sigma$. Solution 2.)



Re $D=0$
Im $D=0$

T-matrix poles:

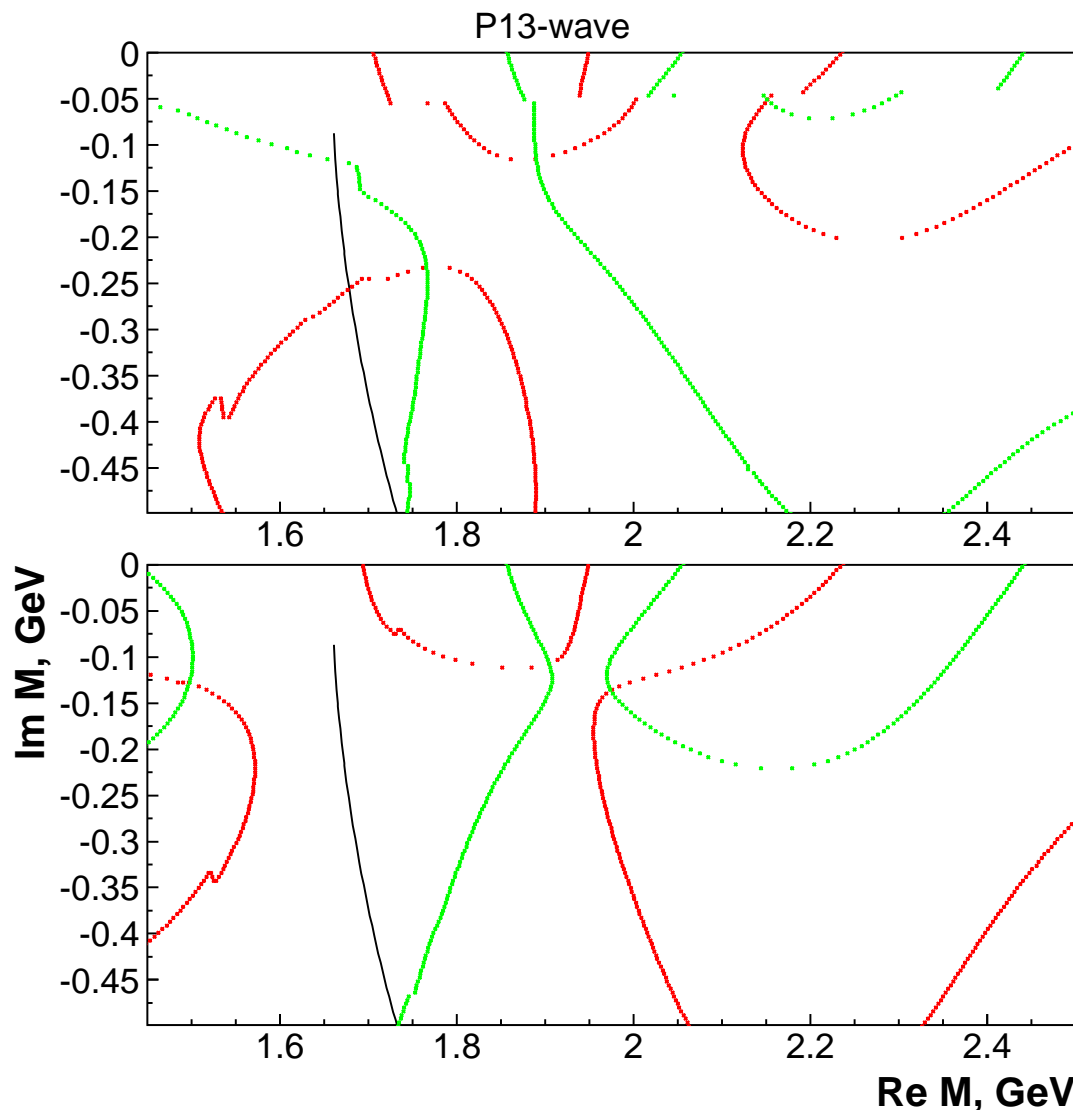
$$M = 1370 - i100 \text{ MeV};$$

$$M = 1695 - i115 \text{ MeV}$$

$$M = 1940 - i220 \text{ MeV}$$

P₁₃: 3-pole 8-channel K-matrix

$(\pi N, \eta N, K\Lambda, K\Sigma, \pi\Delta(1232)(P,F), N\sigma, D_{13}(1520)\pi)$



Re D=0 **Im D=0**

I sheet: closest to the physical region below $D_{13}(1520)\pi$ threshold.
 $M = 1730 - i230$ MeV;

II sheet: closest to the physical region above $D_{13}(1520)\pi$ threshold.
 $M = 1500 - i125$ MeV
 $M = 1900 - i100$ MeV
 $M = 1980 - i140$ MeV

Tabelle 1: Pole position (in MeV), πN , ηN , $K\Lambda$ and $K\Sigma$ couplings (in GeV) and photo-couplings (in $\text{GeV}^{-1/2} 10^3$).

State	$P_{11}(1440)$	$P_{11}(1710)$
Re(pole)	1375 ± 6 (1365 ± 15)	1690^{+25}_{-10} (1720 ± 50)
-2Im(pole)	200 ± 10 (190 ± 30)	230^{+30}_{-20} (230 ± 150)
$g(\pi N)$	0.49 ± 0.03 / $40 \pm 6^\circ$	0.16 ± 0.06 / $(5^{+20}_{-50})^\circ$
$g(\eta N)$	-0.12 ± 0.05 / $20 \pm 10^\circ$	-0.16 ± 0.05 / $20 \pm 25^\circ$
$g(K\Lambda)$		0.70 ± 0.20 / $8 \pm 10^\circ$
$g(K\Sigma)$		0.10 ± 0.05 / $(60^{+60}_{-30})^\circ$
$A^{1/2}(\gamma p)$	-44 ± 10 / $-37^\circ \pm 10^\circ$	-65 ± 25 / $-65^\circ \pm 20^\circ$
State	$P_{11}(1840)$	$P_{13}(1720)$
Re(pole)	1860 ± 10 ()	1720 ± 50 (1675 ± 15)
-2Im(pole)	110^{+30}_{-10} ()	420 ± 80 (190 ± 85)
$g(\pi N)$	0.12 ± 0.04 / $(15^{+15}_{-25})^\circ$	0.78 ± 0.12 / $35 \pm 10^\circ$
$g(\eta N)$	-0.46 ± 0.10 / $25 \pm 12^\circ$	0.75 ± 0.15 / $15 \pm 10^\circ$
$g(K\Lambda)$	$-(0.07^{+0.10}_{-0.05})$ / $0^{+12}_{-22} \circ$	0.60 ± 0.35 / $15 \pm 20^\circ$
$g(K\Sigma)$	0.30 ± 0.10 / $40^{+60}_{-30} \circ$	1.15 ± 0.60 / $10 \pm 10^\circ$
$A^{1/2}(\gamma p)$	-14 ± 6 / $50^\circ \pm 50^\circ$	160 ± 30 / $25^\circ \pm 35^\circ$
$A^{3/2}(\gamma p)$		150 ± 60 / $50^\circ \pm 40^\circ$

Tabelle 2: Pole position (in MeV), πN , ηN , $K\Lambda$ and $K\Sigma$ couplings (in GeV) and photo-couplings (in $\text{GeV}^{-1/2} 10^3$).

State	$P_{13}(1960)$	$P_{13}(1900)$
Re(pole)	$1970 \pm 12 (\sim 1900)$	$1890 \pm 50 ()$
-2Im(pole)	$300 \pm 60 ()$	$270^{+200}_{-100} ()$
$g(\pi N)$	$0.13 \pm 0.20 / 20 \pm 50^\circ$	$0.15 \pm 0.10 / (20^{+50}_{-100})^\circ$
$g(\eta N)$	$-0.70 \pm 0.20 / 5 \pm 15^\circ$	$-(0.40^{+0.40}_{-0.30} / (5^{+70}_{-50}))^\circ$
$g(K\Lambda)$	$-(1.10^{+0.50}_{-0.30}) / 0 \pm 15^\circ$	$-0.70 \pm 0.35 / (5^{+70}_{-35})^\circ$
$g(K\Sigma)$	$-0.40 \pm 0.15 / (35^{+15}_{-30})^\circ$	$0.40^{+0.50}_{-0.25} / (5^{+40}_{-100})^\circ$
$A^{1/2}(\gamma p)$	$9 \pm 7 / 2 \pm 10^\circ$	$63 \pm 20 / 65^\circ \pm 20^\circ$
$A^{3/2}(\gamma p)$	$50 \pm 40 / 55^\circ \pm 40^\circ$	$63 \pm 15 / 80^\circ \pm 30^\circ$
State	$P_{33}(1600)$	$P_{33}(1920)$
Re(pole)	$1480 \pm 40 (1550 \pm 100)$	$1925 \pm 40 (1900 \pm 50)$
-2Im(pole)	$230 \pm 40 (300 \pm 100)$	$320 \pm 50 (300 \pm 100)$
$g(\pi N)$	$0.40 \pm 0.10 / 85 \pm 15^\circ$	$0.45 \pm 0.15 / -30 \pm 25^\circ$
$g(K\Sigma)$	$-0.15 \pm 0.08 / -15 \pm 15^\circ$	$-0.20 \pm 0.10 / 20 \pm 15^\circ$
$A^{1/2}(\gamma p)$	$20 \pm 12 / 55^\circ \pm 20^\circ$	$100 \pm 20 / -55^\circ \pm 15^\circ$
$A^{3/2}(\gamma p)$	$14 \pm 10 / -5^\circ \pm 20^\circ$	$-73 \pm 12 / 35^\circ \pm 15^\circ$

Summary

1. Analysis of the $\pi^- p \rightarrow K^0 \Lambda$ reaction confirms firmly the $P_{11}(1710)$ state. It also confirms existence of the $P_{11}(1860)$ state however there are two solutions which give very different widths for this state.
2. The data on $\pi^+ p \rightarrow K^+ \Sigma^+$ confirm the $P_{33}(1600)$ and $P_{33}(1920)$ resonances.
3. The fit of new polarization observable I_c on $\gamma p \rightarrow \eta \pi^0 n$ confirms the solution published in Eur.Phys.J.A38:173-186,2008: $D_{33}(1980)$.
4. The combined analysis of pion- and photoproduction reactions confirms the $P_{13}(1900)$ state. Moreover, there is a strong indication for a double pole structure in this region.
5. The new data on the $\gamma p \rightarrow K \Lambda$ reaction (CLAS: $d\Sigma/d\Omega$, \mathbf{P} ; GRAAL: O_x, O_z, T) shows an indication for the third S_{11} state with mass 1890 ± 10 MeV and width 90 ± 10 MeV.

Problem: how to compare our results with other analyses?

For example with Breit-Wigner parameters given in PDG.

We construct the following amplitude:

$$A_{ij}^{BW} = \frac{g_i^{BW} g_j^{BW}}{M_{BW}^2 - s - i\beta \sum_i g_i^2 \rho_i}$$

where M_{BW} and β are fitted to reconstruct pole position and g_i^{BW} to reconstruct residues in the pole.

As a cross-check: the procedure works very well for the relativistic Breit-Wigner amplitude

$$(g_i^{BW})^2 \sim \beta g_i^2$$

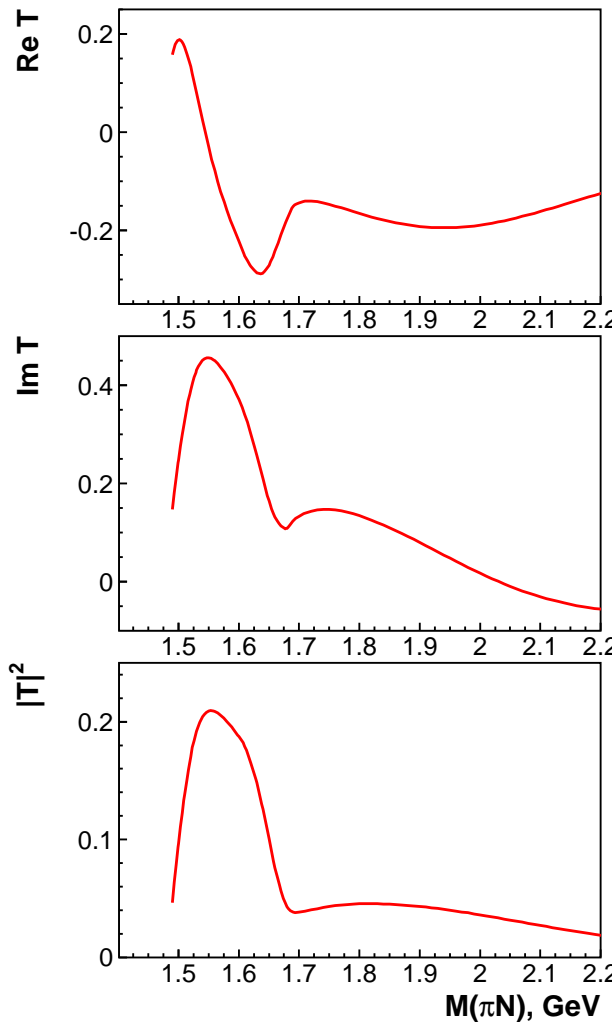
and width can be estimated as:

$$M_{BW} \Gamma_{tot}^{BW} = Im(i\beta \sum_i g_i^2 \rho_i)$$

S11-wave transition amplitudes

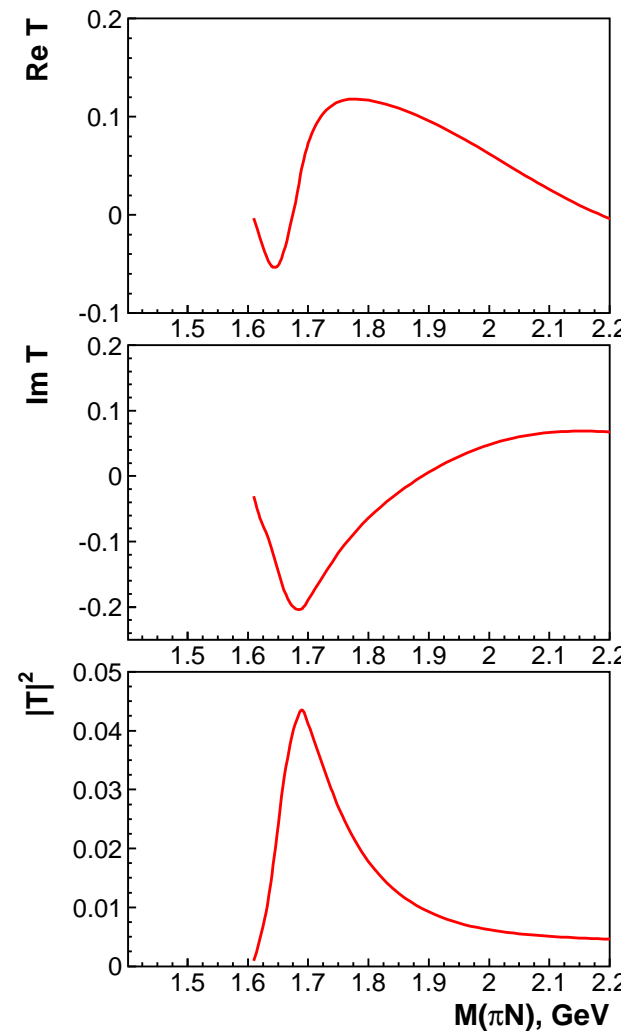
$\pi N \rightarrow \eta N$

S11-wave



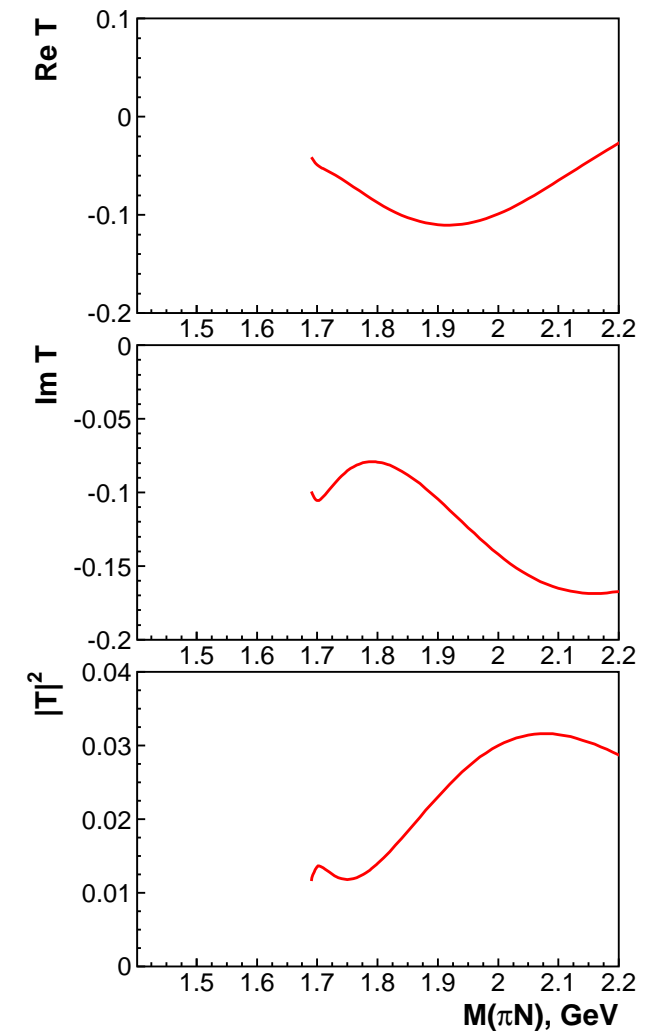
$\pi N \rightarrow K\Lambda$

S11-wave

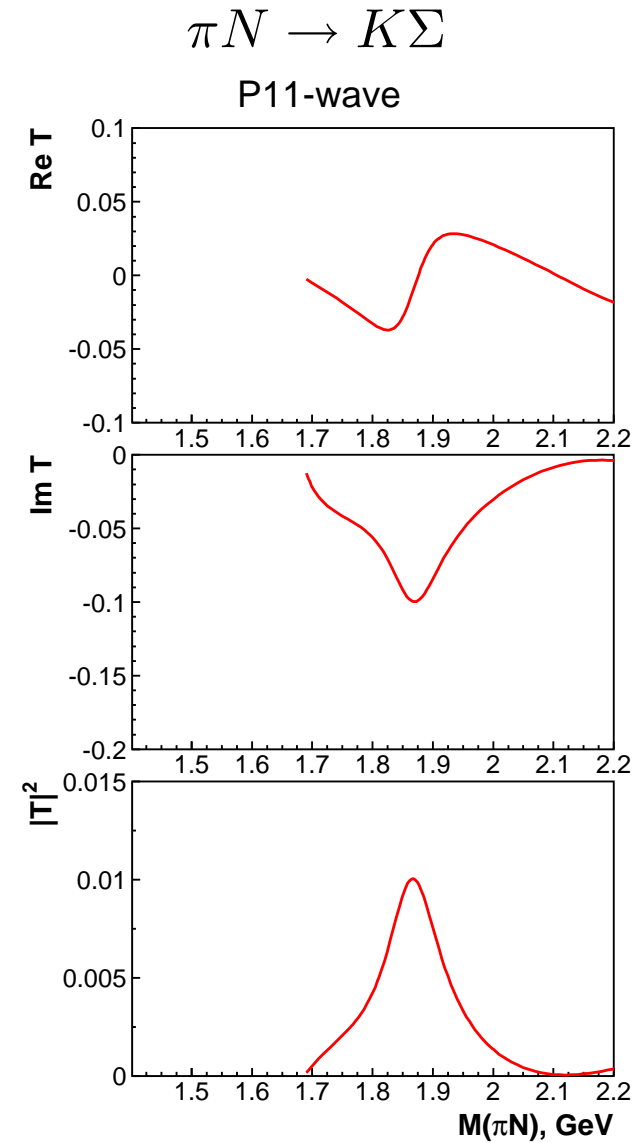
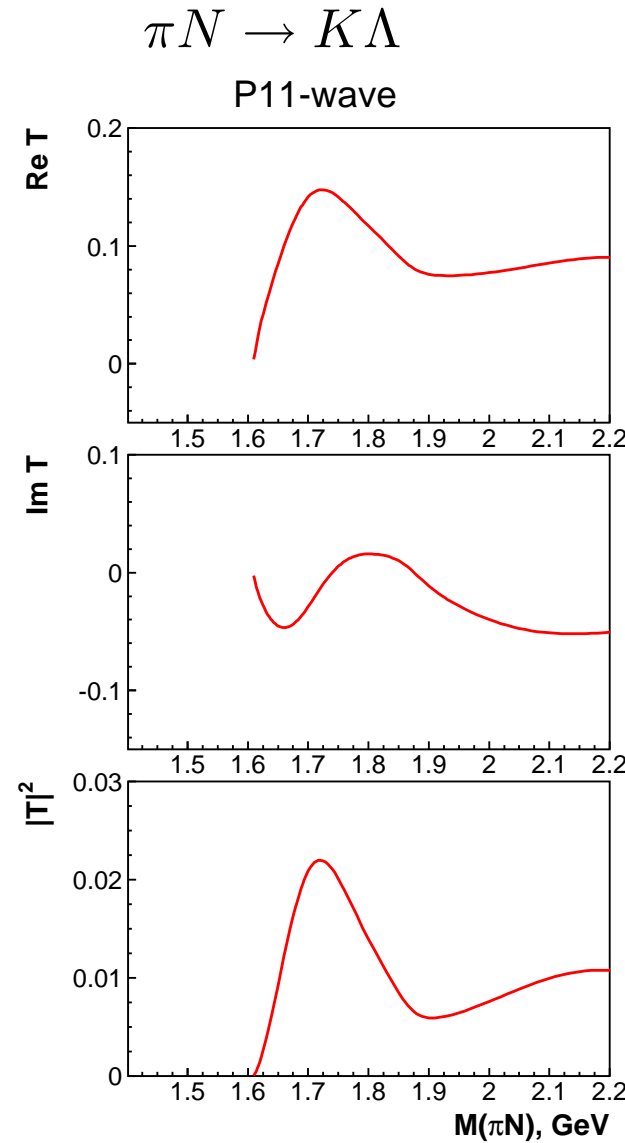
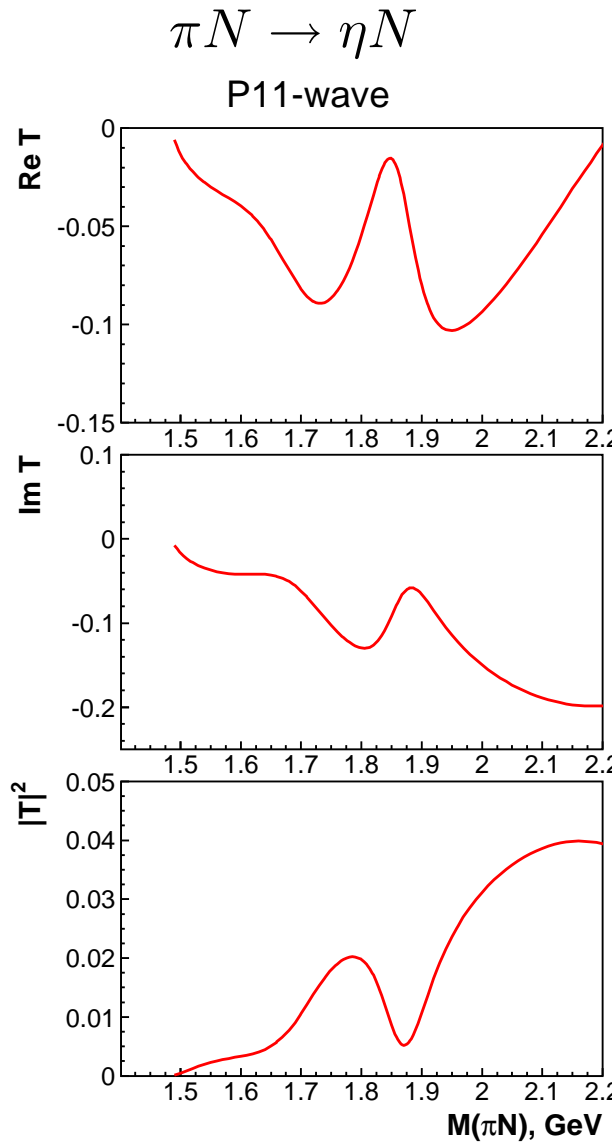


$\pi N \rightarrow K\Sigma$

S11-wave

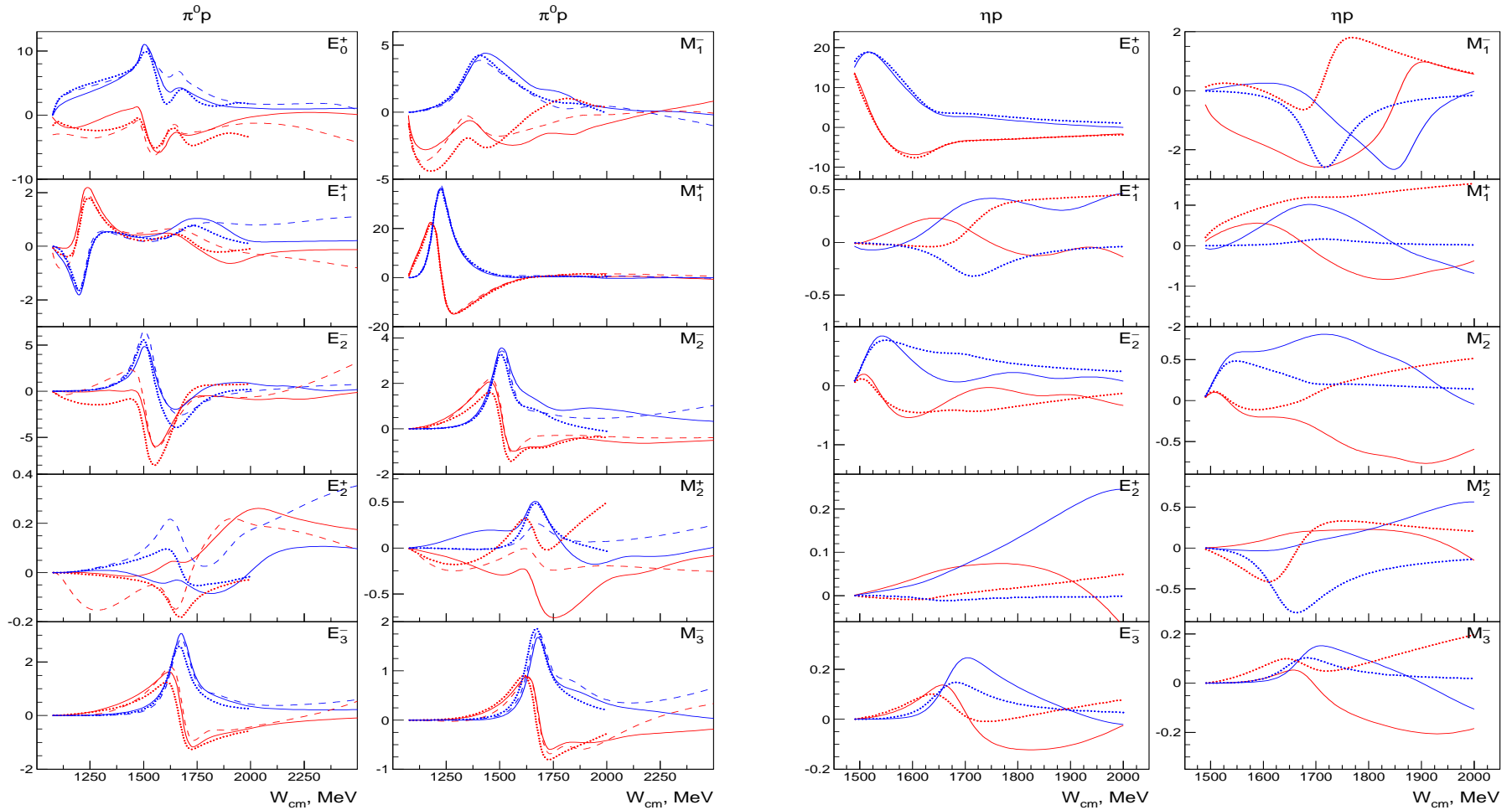


P11-wave transition amplitudes

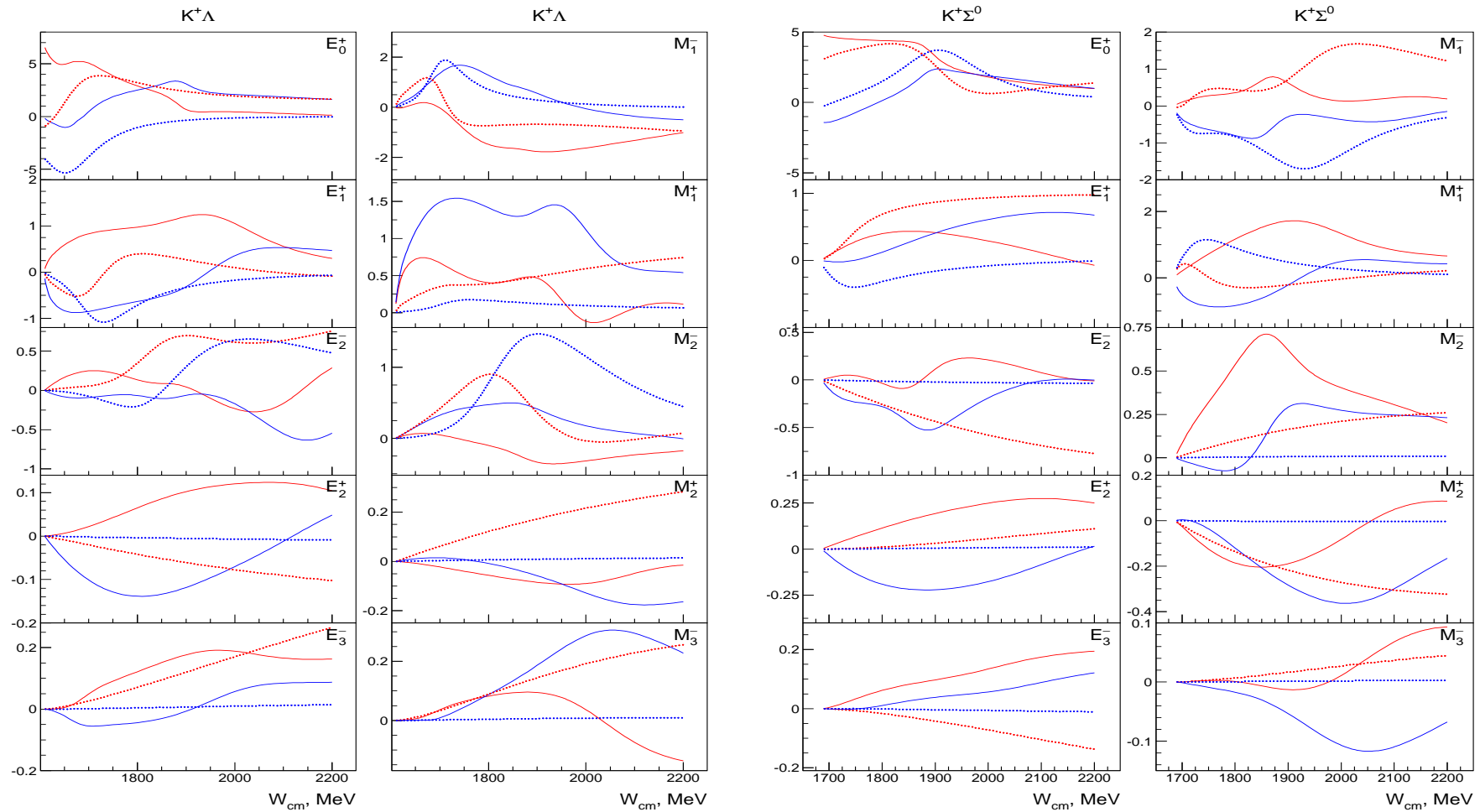


Multipoles for the single π^0 and η production. Red - real part, Blue - imaginary part.

Solid curves is our solution, dashed curves - SAID solution, dotted - MAID 2009.



Multipoles for the $K\Lambda$ and $K\Sigma$ final states. Red - real part, Blue - imaginary part. Solid curves is our solution, dashed curves -- MAID 2009.



N/D based analysis of the data

In the case of resonance contributions only we have factorization and Bethe-Salpeter equation can be easily solved:

$$\text{J} \quad m = \text{J} \quad K \quad \begin{matrix} \pi \eta K \\ \pi \eta K \end{matrix} \quad m + \delta_{JK}$$

$$A_{jm} = A_{jk} \sum_{\alpha} B_{\alpha}^{km}(s) \frac{1}{M_m - s} + \frac{\delta_{jm}}{M_j^2 - s} \quad B_{\alpha}^{km}(s) = \int_{4m_j^2}^{\infty} \frac{ds'}{\pi} \frac{g_{\alpha}^{(k)}(s') \rho(s') g_{\alpha}^{(m)}(s')}{s' - s - i0}$$

$$\hat{A} = \hat{\kappa} (I - \hat{B} \hat{\kappa})^{-1} \quad \kappa_{ij} = \frac{\delta_{ij}}{M_i^2 - s} \quad B^{ij} = \sum_{\alpha} B_{\alpha}^{km}(s)$$

For non-resonant contributions: there is no factorization and the amplitude can have a complicated energy dependence. However in majority of K-matrix analysis the nonresonant contributions are constant or have a simple energy dependence.

Non-factorization can be taken into account by introduction of two transitions with fixed left and right vertices.

Parameterization of P_{13} wave: 3 resonances 8 channels, 4 non-resonant contributions
 $\pi N \rightarrow \pi N, \pi N \rightarrow \eta N, \pi N \rightarrow K\Sigma, \pi N \rightarrow \Delta\pi$. It corresponds to **8 × 8 channel K-matrix** and **5 × 5 N/D-matrix**.

In many cases (fixed form-factor or subtraction procedure) the real part can be calculated in advance (for S-wave):

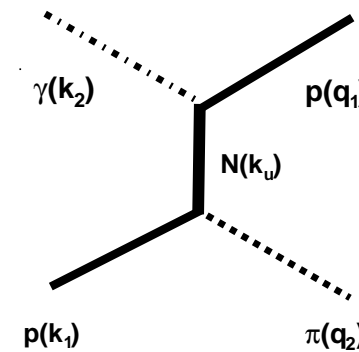
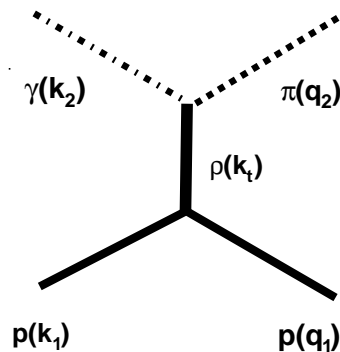
$$B(s) = \text{Re}B(M^2) + \frac{g^2}{\pi} [\rho(s) \ln \frac{1 - \rho(s)}{1 + \rho(s)} - \rho(M^2) \ln \frac{1 - \rho(M^2)}{1 + \rho(M^2)}] + i\rho(s)g^2$$

The P-vector approach is strait forward:

$$A_{ab} = \sum_{ij} \quad \begin{array}{c} i \\ \diagup \quad \diagdown \\ a \bullet \text{---} \text{---} \text{---} \bullet b \\ | \qquad \qquad | \\ j \end{array} \quad P_b = \sum_{ij} \quad \begin{array}{c} i \\ \diagup \quad \diagdown \\ a \bullet \text{---} \text{---} \text{---} \bullet b \\ | \qquad \qquad | \\ j \\ \text{---} \text{---} \text{---} \text{---} \text{---} \text{---} \text{---} \text{---} \end{array}$$

1. This approach satisfies analyticity and two body unitarity conditions. It takes left-hand side singularities into account.
2. The approach is suitable for the analysis of high statistic data in combined analysis of many reactions.
3. However: a treatment of the real part for interfering resonances is model dependent.

Reggeized exchanges:



The amplitude for t-channel exchange:

$$A = g_1(t)g_2(t)R(\xi, \nu, t) = g_1(t)g_2(t) \frac{1 + \xi \exp(-i\pi\alpha(t))}{\sin(\pi\alpha(t))} \frac{\nu}{\nu_0}^{\alpha(t)} \quad \nu = \frac{1}{2}(s - u).$$

Here $\alpha(t)$ is Reggeon trajectory, and ξ is its signature:

$$R(+, \nu, t) = \frac{e^{-i\frac{\pi}{2}\alpha(t)}}{\sin(\frac{\pi}{2}\alpha(t))\Gamma_{-\frac{\alpha(t)}{2}}} \frac{\nu}{\nu_0}^{\alpha(t)},$$

$$R(-, \nu, t) = \frac{ie^{-i\frac{\pi}{2}\alpha(t)}}{\cos(\frac{\pi}{2}\alpha(t))\Gamma_{-\frac{\alpha(t)}{2} + \frac{1}{2}}} \frac{\nu}{\nu_0}^{\alpha(t)}.$$